Order Number 1341568

Later aftershocks of the March 2, 1987 Edgecumbe, New Zealand, earthquake

Zhang, Jianjun, M.S.

University of Nevada, Reno, 1990

UMI
300 N. Zeeb Rd.
Ann Arbor, MI 48106

University of Nevada-Reno

Later Aftershocks of the March 2,1987 Edgecumbe, New Zealand, Earthquake

A Thesis submitted in partial fulfillment of the requirements for the degree of Master of Science in Geophysics

BY

JIANJUN ZHANG

May 1990

The thesis of Jianjun Zhang is approved:

Thesis Adviser

Department Chairman

Graduate Dean

University of Nevada-Reno

May 1990

Acknowledgement

The author of this thesis wishes first to thank Dr. John Anderson for his precious academic advice on the study in this thesis and for his various kind support during the study. This study would be impossible without his support.

The author of this thesis also thanks Dr. James N. Brune and Dr. R. Siddharthan for their willingness to participate in the graduate committee. Specially the author thanks Dr. James N. Brune for the financial support in the course of the study.

Finally thanks go to Geoffrey King and Keith Priestley for their generously providing data to this study. The author very much appreciates the discussion with Dr. William Peppin and thanks him for providing help on computer facilities.

This research was completed with partial support from the State of Nevada Nuclear Waste Project Office.

Later Aftershocks of the March 2, 1987 Edgecumbe, New Zealand, Earthquake

ABSTRACT

The March 2, 1987 Edgecumbe, New Zealand earthquake had a magnitude (M_L) 6.3 and seismic moment $7.0*10^{18}$ N*m. Later aftershocks, from March 15 to 27, were monitored with 10 portable smoked paper recorders operated by the United States Geological Survey, and by seven digital event recorders from the University of Nevada, Reno. Two magnitude scales for these aftershocks were established by calibration of amplitudes and coda durations with seismic moments determined from digital records for 18 events. Most events analyzed have magnitudes between 1.0 and 2.8.

Aftershocks form a zone at least 50 km long striking about N40°E. In the southwestern part, the epicenters are in a narrow zone (<7 km) which broadens to over 15 km wide in the northeast. The depth distribution peaks at 6 km, and most of the events are between 3 and 11 km. A gap in the epicenter distribution near Mt. Edgecumbe suggests the high temperature in that area. Both the depth distribution and epicenter distribution are consistent with the geology of the region: the area has a thin crust and high heat

flow which is a consequence of back arc spreading.

Focal mechanisms indicate predominantly normal faulting with a small strike slip component. Fault strikes are consistent with the trend of the epicenter distribution, with an extension axis which is about N145°E. The preferred fault planes are often ambiguous, but when combined with geological data they are consistent with a dip angle 50 degree downthrown northwest in the northern part of rupture. In the southern part, a southeasterly dip may be preferable. Some mechanisms which deviate from this trend imply the geological complexity in the region.

Table of Contents

Title page..i

Signature page......................................ii

Acknowledgement.....................................iii

Abstract..iv

Table of contents...................................vi

Table of figure and table captions..................vii

INTRODUCTION..1

GEOLOGICAL SETTING..................................5

DATA COLLECTION.....................................9

HYPOCENTER LOCATIONS................................12

FOCAL MECHANISM ANALYSIS............................22

CONCLUSION..35

REFERENCES..50

Table of Figure and Table Captions

Figure Captions:

Figure 1 -- Major surface ruptures in 1987 Edgecumbe earthquake and Rangitaiki Plain........................2

Figure 2 -- Central Volcanic Zone and North Island Shear Belt..................6

Figure 3 -- Station sites and later aftershock epicenters (Mar.15-27).........11

Figure 4 (a-m) -- Aftershock epicenters day by day from Mar.15 to Mar.27................19-31

Figure 5a -- Cross section distribution along AA'......36

Figure 5b -- Cross section distribution along BB'......37

Figure 5c -- Cross section distribution along CC'......38

Figure 5d -- Cross section distribution along DD'......39

Figure 6a -- Coda duration magnitude vs moment and moment magnitude.....................40

Figure 6b -- Amplitude magnitude vs coda duration magnitude..................41

Figure 7 -- Magnitude vs time........................42

Figure 8 -- Histogram (Mar.15-27)....................43

Figure 9 -- Focal Mechanism of four aftershock clusters......................48

Table Captions:

Table 1 -- Velocity model used in hypocenter locating........................14

Table 2 -- Aftershock event list.....................15-18

INTRODUCTION

The March 2, 1987 Edgecumbe earthquake occurred near the northeastern shore of the North Island of New Zealand. The main shock had magnitude M_L 6.3, seismic moment $M_0 = 7*10^{18}$ N*m [Priestley 1989], and focal depth 8 Km for the main shock [Anderson and Webb 1989]. The focal mechanism based on body waves indicated predominantly normal faulting (Staff of New Zealand Department of Scientific and Industrial Research 1987, Anderson & Webb 1989). But normal mode analysis indicated an important strike slip component was also present (Priestley 1989). The observed surface ruptures after the earthquake also revealed both normal and strike slip components (Geoffrey King 1989, personal communication, Beanland at al 1989). The maximum vertical offset on the ground surface due to the main shock was measured as 2.5 m and the average was 1.4 m on the Edgecumbe fault. An eyewitness saw the rupture propagating from northwest to southeast on the Edgecumbe fault during the main shock [Beanland at al 1989]. Soon after the earthquake a systematic field survey was carried out by the Department of Scientific and Industrial Research, New Zealand, as well as other geological institution like United States Geological Survey. More than 10 surface ruptures due to this earthquake were observed (Figure 1). Some ruptures occurred on pre-existing but previously unrecognized fault scarps, while some others were new surface breaks. Most of the observed surface ruptures had a strike trending northeast

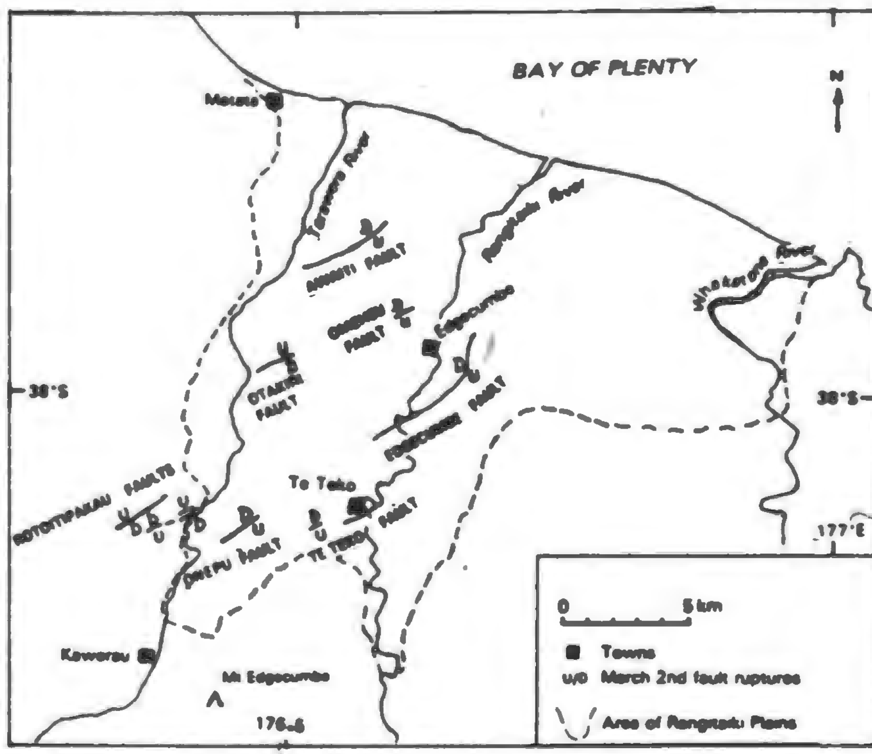

Fig.1 - Major faults, surface ruptures and Rangitaiki Plain.
(after Beanland et al 1989)

downthrown to the northwest, while a small number of ruptures were downthrown to the southeast (Fig 1). The longest rupture was 7 km and the shortest 0.5 km. The pre-existing Edgecumbe fault trace had the most significant surface rupture.

The Edgecumbe earthquake occurred in the Whakatane Graben which is at the northeast corner of Central Volcanic Region. The Central Volcanic Zone extends from the central part of the North Island north to the ocean. This extensional region has been explained as the on-land expression of a young oceanic back arc basin which extends to the north behind the Kermadec subduction zone (Stern 1985). The zone has a high heat flow, and mostly shallow earthquakes, but also some deeper events on the subduction zone. All historical earthquakes in this region have had magnitudes less than 7. The corresponding segment of the Kermadec subduction zone, east to the Central Volcanic Zone, experienced a magnitude 8 earthquake in 1931 (Hawkes Bay earthquake). The Central Volcanic Zone has large, normal faults on both its eastern and western boundaries. Most of the recent seismic activity in the Central Volcanic zone has not involved these faults, and has mostly been associated with volcanic events. The Edgecumbe earthquake neither involved faulting on the main boundary faults, nor was it closely associated with volcanic activity. Rather the surface expression primarily involved smaller faults central to the Whakatane graben.

The Edgecumbe earthquake was perhaps the most significant earthquake in New Zealand in the past two decades. There was extensive damage in the towns of Edgecumbe and Te Teko, and an important set of strong motion accelerograms was obtained. The earthquake provided an opportunity to study the expression of a back arc system on land.

After the main shock on Mar 2, portable seismic recorders were installed and operated by seismologists from Department of Scientific and Industrial Research, Wellington, New Zealand, from the Seismological Laboratory, University of Nevada-Reno and from the United States Geological Survey, Golden, Colorado. In this paper we study the later aftershock data (from Mar 15 to Mar 27) primarily as recorded on ten portable smoked drum recorders operated by USGS, and supplemented by records from seven digital recorders operated by the University of Nevada-Reno, to investigate the rupture properties and the focal mechanism of the source.

GEOLOGICAL SETTING

New Zealand is on the boundary between the Pacific and Indian plates. Along the eastern coast of North Island the Pacific plate is thrusting under the Indian plate. Two major tectonic features of North Island are North Island Shear Belts and the Central Volcanic Zone (Figure 2). The shear belt strikes south-north across North Island. It consists of several active right-lateral strike-slip faults with relatively small reverse components. The quantitative slip rate was estimated as 14 mm/year of strike slip and 4 mm/year of reverse slip [Sisson 1979, Nairn & Beanland 1989]. The northern end of the shear belt intersects the northeastern part of Central Volcanic Zone at the Whakatane graben where the 1987 Edgecumbe earthquake occurred. The severe 1866 earthquake, which was the last strong earthquake before the 1987 Edgecumbe earthquake in the Whakatane graben, was suspiciously related to one of major faults of the belts but the earthquake was only described in a story and lacked data to make it fully explained [Nairn & Beanland 1989].

The other important feature of north island is the Central Volcanic Zone (CVZ). This region is shaped like a sector with origin at heart of the island and diverging to north. It is an extensional environment with extremely high heat flow (about 700-800 mW/m^2 [Studt & Thompson 1969]). The CVZ consists of a huge volume of Quaternary rhyolitic volcanic rocks (estimated as about 12,000 km^3 [Cole 1979]). The CVZ was explained as a back arc

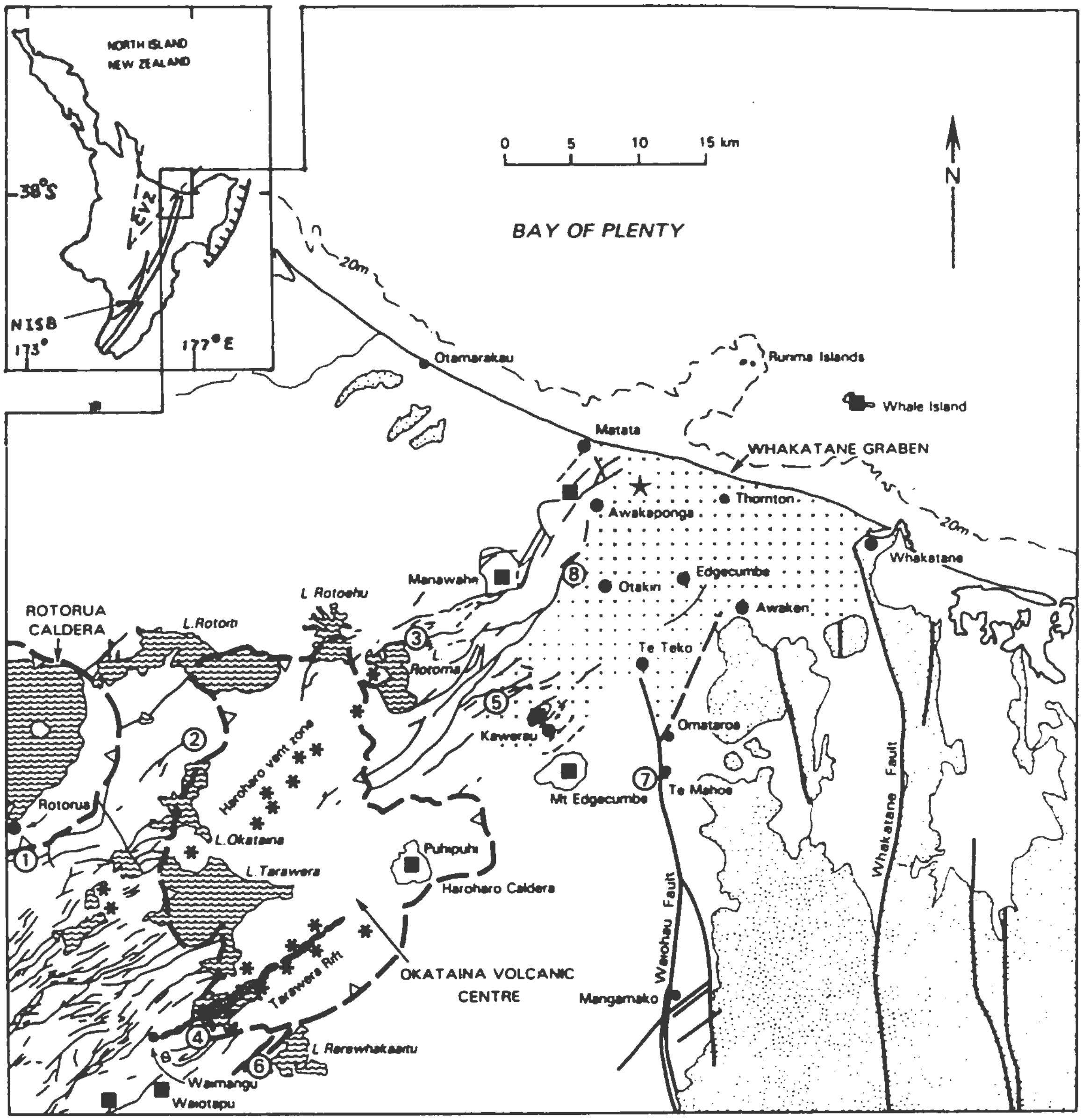

Fig.2 - Central Volcanic Zone and North Island Shear Belts. (after Nairn & Beanland 1989)

Tectonic map of the Bay of Plenty region showing relationship of Whakatane Graben, Okataina Volcanic Centre, and fault traces of the Taupo Fault Belt and North Island Shear Belt. Symbols as for Fig. 1. 1 Horohoro Fault; 2 Whakapoungakau Fault; 3 North Rotoma Fault; 4 Rotomahana Fault; 5 Rotoitipakau Fault Zone; 6 Rerewhakaaitu fissures; 7 Matahina Dam; 8 Braemar Fault. Faults shown within Whakatane Graben are pre-1987 traces.

spreading center behind the Kermadec trench along the east coast and was recognized as the continuation of a subsidence trough right off coast in the Bay of Plenty [Stern 1978]. The average crust thickness in CVZ is only about 15 km [Stern 1985]. Of more tectonic significance is the eastern part of the CVZ, called Taupo Volcanic Zone (TVZ) which contains numerous active small faults and recent volcanism. In some places in the TVZ, for example Tarawera and Waimangu, one finds the eruption of basalt, with origin in the mantle. Thus one might expect faults dominated by near vertical and dike eruption fractures. But the intrusive volcanic vents do not correspond to the observed fault traces. Furthermore, many faults have a dip angle of 45°-55°, and can only be explained as the result of normal faulting instead of dike eruption. From the investigation of pyroclastic deposits which were already dated [Nairn 1976], it is concluded that most of the faults in northern TVZ had repeated displacements in the recent 50,000 years. The last significant displacement occurred about 1850 years ago by indication of the Taupo pumice deposit.

The 1987 Edgecumbe earthquake occurred in the Whakatane graben. Whakatane graben is at the northern end of TVZ. In the 20 km wide graben, the greywacke basement subsided 2 km below sea level by the interpretation of gravity contours [Nairn & Beanland 1989]. The graben is filled with volcanic ashes and marine deposits of Holocene sediments which formed todays Rangitaiki Plain. Geodetic surveys covering the northern part of TVZ gave a spreading rate of 7 mm/year [Sisson 1979, Nairn & Beanland 1989]. Most of this spreading was contributed by the TVZ normal faults within the Whakatane graben. From geothermal drillholes, an estimation of the average subsidence rate of the Whakatane graben is around 1 mm/year. Close to the graben axis it reached 2-3 mm/year during past 5500 years [Pullar 1981, Nairn & Beanland 1989]. While the graben was subsiding and was extending horizontally its margin was uplifting. The marine sediments with age of 120,000 years at the eastern margin and the Matahina ignimbrite with age of 290,000 years were uplift about 60 m and 300 m respectively; they are considered to have been deposited at the same level as today's sea level. So, from comparing Quaternary marine sediments or the Matahina ignimbrites obtained from geothermal drillholes the uplift of graben margins was estimated as 0.5 mm/year for eastern margins and more than 1 mm/year for western margins [Nairn & Beanland 1989]. The mechanism of uplift in such an extensional graben environment was likely explained by the intrusion of magma underneath, but it is still not certain [Nairn & Beanland 1989].

The 1987 Edgecume earthquake was the continuation of the process of Whakatane graben subsiding and extending. This process has been going on since Mid-Quaternary period. It is generally recognized that the Edgecumbe fault within the graben played a major role in the 1987 Edgecumbe event. Study of the Taupo Pumice deposit at the Edgecumbe fault indicated two major events within the last 1850 years; one was about 800 years ago [Nairn & Beanland 1989, Beanland at al 1989]. They suggest that the major earthquake cycle on the Edgecumbe fault would be near 1000 years.

DATA COLLECTION

Ten portable smoked paper recorders were distributed as in figure 3. All of these recorders were short period vertical seismometers and worked with a paper speed of 1 mm per second. The clock calibration was read every time recording paper was changed (about 48 hours per sheet of recording paper). Typically the clock drift is about 20 - 40 millisecond per 48 hours. Those clock calibrations were taken into account by linear interpolation for aftershock locating. On average, each located event was effectively recorded by 4 to 8 stations. Major factors which prevented more complete recording included trace obscured by larger events, small amplitudes caused by far distance between event and station, and occasional mechanical problems of recorders. As many aftershock events were picked as possible but many of these events could not located unambiguously.

In order to increase record reading resolution a microscope with a magnifying power 20 was used to read the smoked paper records. The resolution with such a microscope can easily reach 0.025 mm. Since every millimeter on the recording paper represented 1 second that resolution means reading accuracy of 25 millisecond was achieved. P arrivals were usually very obvious and can generally be picked up with the above accuracy. S arrivals were of course often difficult or ambiguous to identify, and in many cases they were not identified at all. Also read at the same time was the first arrival polarity Up or Down of the event, for focal mechanism analysis. Two parameters were read for magnitude estimation: the peak to peak amplitude and the signal duration. Both were read by a digital caliper and the reading accuracy was about 0.5 millimeter.

Fig.3 Station sites and later aftershock epicenters.

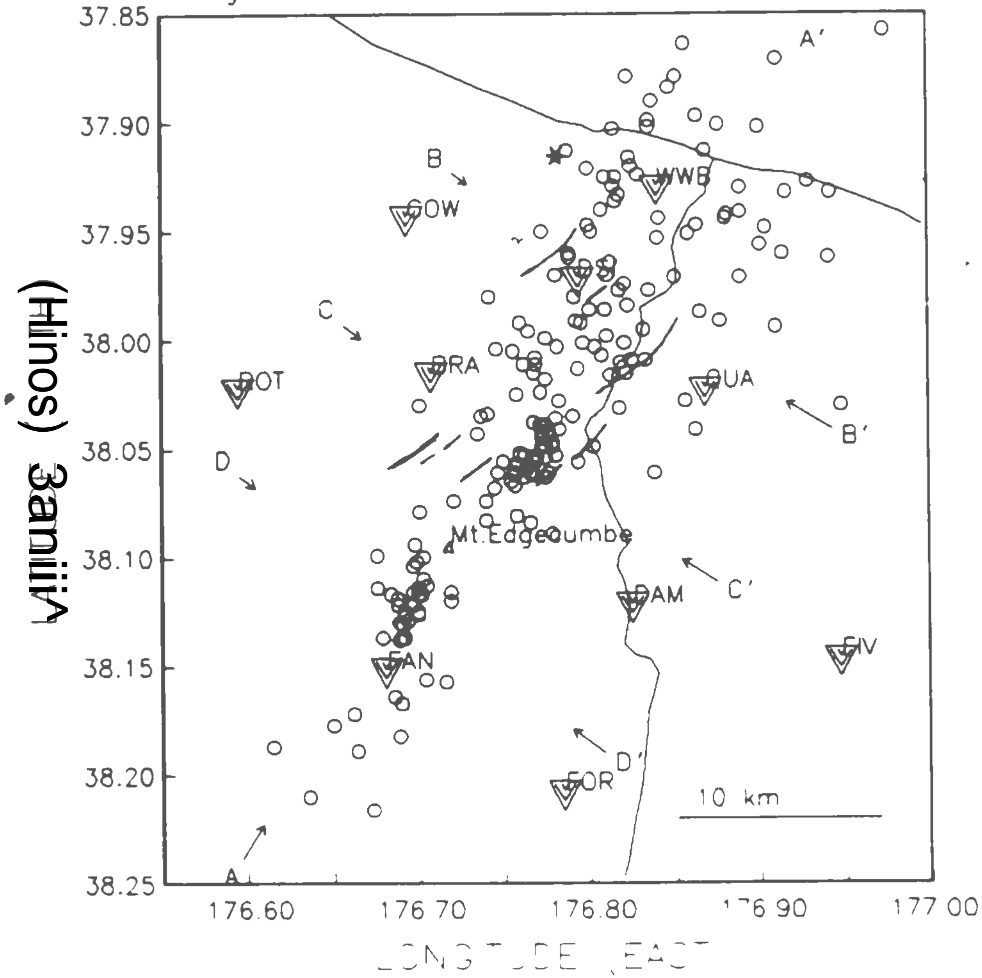

HYPOCENTER LOCATIONS

The program HYPOINVERSE [Klein 1978], which uses an inversion method via singular value decomposition, was used to locate all the aftershocks in our study. Only events with relatively reliable locations, which had a vertical uncertainty (in sense of one standard deviation) less than 5 km and had at least 4 stations participated effectively in locating, were used in our analysis. The velocity model was the same Edgecumbe model as used by Robinson in his study of early aftershock locations [Robinson 1989], and is listed in Table 1. This velocity model was derived using 38 well-recorded events with a method that estimated hypocenters and velocity model simultaneously [Crosson 1976]. All the epicenter locations are shown in Figure 3. The mark (*) is the main shock. Table 2 lists all later aftershocks we located, where ORIGIN is the event origin time (year-month-day-hour-minute and second); LAT and LON are the latitude (^{o}S) and longitude (^{o}E) of located epicenter; DEPTH is focal depth; RMS is root of mean weighted squared error of residual between observed and calculated arrival time in second; ERH and ERZ are horizontal and vertical uncertainty under one standard deviation; GAP is the largest sector in degree that stations didn't cover in locating and the smaller the GAP the better the location; Ma and Mc are amplitude and coda duration magnitude and finally the ESN is the effective station number under which the first digit means the effective stations used in locating and the digit after letter S means how many S arrivals are effectively used in locating, which could affect the reliability of deep hypocenter locations. Usually in our case horizontal uncertainties are about the same size as vertical uncertainties.

Table 1 (Velocity Model)

Depth (km)	P Velocity (km/sec)
0.0 - 1.0	2.40
1.0 - 6.0	5.00
6.0 - 10.0	5.91
10.0 - 15.0	6.55
15.0 -	7.50

Table 2 (Aftershock Event List)

No.	ORIGIN	YMDHM_Sec		LAT S	LON E	DEPTH	RMS	ERH	ERZ	GAP	Ma	Mc	ESN
1	87	3150029	6.32	37.970	176.811	4.2	.08	1.6	.5	245	2.3	2.3	4S1
2	87	3150239	41.55	37.879	176.851	14.6	.20	2.9	.7	291	2.1	1.9	5S2
3	87	3151730	10.98	38.172	177.014	16.1	.00	2.1	1.0	289	2.2	1.9	4S0
4	87	3160843	45.66	37.984	176.823	4.5	.00	.1	.2	135	2.1	2.4	5S0
5	**87**	**3160953**	**13.27**	37.986	176.810	8.9	.24	1.5	3.9	124	2.2	2.3	6S2
6	87	3161813	23.17	37.879	176.823	13.2	.14	1.9	.7	287	2.5	2.3	5S1
7	87	3161852	14.24	37.902	176.835	12.2	.22	1.5	2.5	281	2.2	2.1	5S2
8	87	3170040	56.43	37.996	176.765	4.5	.00	.4	.2	237	2.4	2.6	4S0
9	87	3170042	36.04	37.960	176.789	4.3	.03	.2	.3	163	2.3	2.5	5S0
10	87	3170103	50.87	37.921	176.800	9.7	.12	3.1	1.8	208	2.0	1.9	6S1
11	87	3170137	18.22	37.383	178.298	6.4	1.05	3.1	1.8	341	3.0	2.0	4S0
12	87	3170359	35.71	37.950	176.773	3.9	.26	1.2	1.6	152	2.1	2.3	7S0
13	87	3170449	28.16	37.947	176.800	5.2	.01	11.8	3.6	231	1.6	1.7	4S0
14	87	3170550	.25	37.962	176.789	3.8	.04	.2	.4	126	1.8	2.0	6S0
15	87	3170629	28.20	38.091	176.548	4.6	.12	2.9	.8	266	2.2	2.0	6S0
16	87	3171103	12.59	37.992	176.796	4.0	.27	.7	1.7	88	1.9	2.2	6S1
17	87	3171115	23.47	37.899	176.835	6.4	.31	8.3	3.9	271	2.4	2.8	7S0
18	87	3171412	10.51	38.061	176.747	.0	.08	.3	.5	138	1.8	1.6	4S1
19	87	3171619	26.00	37.960	176.914	6.1	.13	1.7	4.0	232	1.8	1.9	4S1
20	87	3172028	6.50	38.034	176.741	5.4	.28	1.2	1.6	109	1.9	1.9	6S0
21	87	3172226	53.80	37.950	176.802	4.6	.04	.5	.3	228	1.7	1.8	5S0
22	87	3180123	16.99	38.119	176.688	.0	.17	.9	1.1	186	2.2	2.0	5S1
23	87	3180301	12.71	37.953	176.840	7.1	.05	1.2	1.8	247	2.2	2.5	5S0
24	87	3180718	59.03	38.024	176.772	7.2	.09	.4	1.0	125	1.9	1.7	6S1
25	87	3180957	24.72	38.035	176.791	5.5	.41	2.5	2.6	94	1.8	2.0	6S0
26	87	3181105	30.03	37.864	176.856	9.7	.08	1.6	.5	286	2.2	1.8	5S1
27	87	3181422	15.28	38.030	176.948	3.8	.00	.4	.2	245	1.9	2.3	4S0
28	87	3181444	20.63	38.041	176.862	4.8	.95	6.5	4.6	134	1.7	1.8	6S1
29	87	3181502	19.78	38.007	176.808	7.5	.05	.5	1.0	160	1.8	1.7	5S0
30	87	3181718	39.86	37.897	176.863	9.4	.07	2.7	.5	285	2.3	1.9	6S0
31	87	3181812	40.12	38.113	176.705	7.0	.04	.5	5.0	171	1.7	1.6	4S0
32	87	3181949	53.88	38.116	176.719	7.4	.01	.2	.7	204	2.2	2.1	5S0
33	87	3182153	26.63	37.890	176.837	7.1	.06	1.6	3.4	276	2.5	2.2	6S0
34	87	3182222	35.62	37.925	176.810	9.4	.03	.7	.4	254	2.2	2.2	5S0
35	87	3190452	16.69	37.916	176.824	7.3	.05	1.2	2.0	261	2.3	2.5	6S0
36	87	3190608	32.63	38.059	176.764	5.7	.08	.4	.4	113	1.8	1.8	6S0
37	87	3190634	27.53	38.120	176.719	7.8	.02	.2	.8	167	2.0	1.8	4S1
38	87	3190723	58.26	37.992	176.760	16.3	.02	2.3	2.6	227	2.0	1.8	4S0
39	87	3190848	59.62	38.004	176.746	10.1	.02	.5	.7	210	1.8	1.6	4S1
40	87	3190907	6.49	38.052	176.760	6.3	.07	.3	1.2	117	1.9	1.9	6S1
41	87	3191107	3.20	37.920	176.825	5.0	.10	.7	.4	258	2.0	1.8	6S2
42	87	3191324	20.32	38.104	176.697	6.9	.00	.2	1.2	170	1.6	1.7	4S0
43	87	3191415	57.99	37.999	176.775	5.7	.06	1.2	.4	213	1.8	1.7	4S1
44	87	3191456	36.84	38.015	176.768	4.6	.05	.2	.4	133	2.0	2.2	6S0
45	87	3191656	35.00	38.049	176.775	6.4	.06	.3	1.1	104	1.9	1.8	7S0
46	87	3191838	35.64	38.005	176.756	15.7	.03	2.5	2.9	204	2.1	1.6	4S0
47	87	3192008	38.98	38.116	176.697	7.1	.00	.3	3.0	178	2.0	1.8	4S0
48	87	3192240	15.59	38.039	176.775	8.5	.13	.6	2.6	141	2.0	1.9	5S1

No.	ORIGIN YMDHM_Sec			LAT S	LON E	DEPTH	RMS	ERH	ERZ	GAP	Ma	Mc	ESN
49	87	3200605	27.56	38.131	176.691	7.7	.01	.3	.4	124	2.1	1.9	4S0
50	87	3200824	8.29	38.089	176.779	2.2	.07	.3	2.8	150	2.0	2.2	6S0
51	87	3201313	50.45	38.129	176.694	7.9	.02	.2	.4	120	2.3	2.1	5S0
52	87	3201315	4.42	38.137	176.692	7.8	.11	1.0	1.5	114	1.7	1.8	4S1
53	87	3201504	7.62	38.100	176.703	6.3	.07	.4	1.4	114	1.9	1.9	5S0
54	87	3201520	22.97	38.216	176.673	5.6	.07	.9	.4	259	2.1	1.8	4S2
55	87	3201559	26.07	38.127	176.692	5.6	.03	.3	.2	188	2.2	2.0	5S0
56	87	3201653	54.07	38.130	176.689	7.5	.06	.4	.8	128	2.3	2.2	6S1
57	87	3201737	47.49	38.122	176.688	5.2	.03	.2	.2	134	2.2	2.2	6S0
58	87	3202330	13.56	37.903	176.815	9.6	.01	2.2	.4	299	2.4	2.0	5S0
59	87	3210451	39.50	38.045	176.773	7.8	.03	.2	.7	131	2.0	1.8	6S0
60	87	3210656	14.70	38.055	176.768	8.1	.04	.2	1.0	115	2.0	1.8	6S0
61	87	3210758	28.72	37.971	176.889	6.6	.06	1.1	.7	267	2.3	2.2	7S0
62	87	3210834	48.67	37.930	176.889	8.7	.06	1.3	.4	278	2.4	2.1	7S1
63	87	3210929	14.89	38.035	176.737	7.4	.06	.9	1.9	129	2.0	1.9	5S0
64	87	3211459	28.54	38.057	176.758	6.6	.03	.1	.6	110	2.1	2.0	7S0
65	87	3211820	25.50	38.094	176.698	3.9	.05	.2	1.6	118	2.1	2.2	7S0
66	87	3211825	50.15	38.079	176.701	9.2	.18	.8	3.2	112	2.4	2.3	7S0
67	87	3211929	56.83	38.003	176.804	5.8	.05	.6	.2	206	1.8	2.0	6S0
68	87	3211946	43.39	37.942	176.881	6.3	.05	1.3	1.7	274	2.3	2.2	7S0
69	87	3211947	45.23	37.940	176.808	7.7	.09	.7	1.4	240	2.0	1.9	5S2
70	87	3212212	23.65	38.065	176.755	5.9	.05	.2	.3	119	1.8	1.7	5S1
71	87	3212308	47.73	38.061	176.757	5.8	.05	.2	.2	104	2.0	2.0	7S0
72	87	3212317	55.87	38.074	176.721	5.6	.28	1.6	1.8	96	1.7	1.8	5S1
73	87	3220802	7.41	38.084	176.766	6.2	.00	.3	.4	239	1.6	1.5	4S0
74	87	3221151	30.01	38.099	176.676	14.4	.24	1.9	4.9	201	2.0	1.6	5S1
75	87	3221237	43.39	37.994	176.910	4.7	.00	.7	.1	299	1.8	1.7	4S0
76	87	3221528	5.40	37.974	176.821	6.6	.00	.2	.3	215	1.5	1.7	4S1
77	87	3221544	16.52	38.114	176.676	3.2	.10	.8	2.8	190	2.3	2.5	8S0
78	87	3221744	3.00	38.053	176.763	5.2	.00	.1	.9	138	1.7	1.5	4S0
79	87	3221750	38.77	38.114	176.700	5.3	.00	.2	.2	212	1.7	1.8	4S0
80	87	3221812	49.94	38.117	176.702	5.8	.05	.3	.3	155	1.8	1.7	6S0
81	87	3222214	12.99	38.062	176.757	5.2	.10	.3	.6	106	2.0	2.1	7S1
82	87	3222216	44.97	37.986	176.801	6.3	.06	.7	1.8	187	2.2	2.2	5S0
83	87	3222252	13.08	38.003	176.782	5.5	.06	.3	.2	154	1.9	2.0	6S0
84	87	3230016	6.70	38.061	176.777	3.3	.06	.2	2.0	90	1.6	1.9	6S0
85	87	3230023	43.04	37.925	176.816	9.3	.04	.3	.4	254	2.0	1.7	5S1
86	87	3230042	45.37	37.956	176.901	6.0	.03	.8	.2	254	2.2	2.1	5S0
87	87	3230125	38.10	38.008	176.769	5.9	.07	.5	.4	142	1.8	1.9	6S1
88	87	3230131	24.78	37.962	176.941	8.3	.02	.3	.6	284	1.9	1.8	4S1
89	87	3230224	57.29	38.042	176.777	.9	.04	.2	.3	138	1.2	1.5	4S1
90	87	3230232	45.23	38.081	176.758	5.6	.19	.6	.8	109	2.1	2.2	6S0
91	87	3230719	16.58	37.884	176.847	8.9	.06	.8	2.4	289	2.0	1.7	4S1
92	87	3230803	8.94	38.126	176.700	5.2	.11	.4	.3	111	2.0	2.1	8S2
93	87	3231035	48.34	38.083	176.740	5.5	.09	.3	.5	125	1.5	1.6	6S2
94	87	3231054	50.19	38.125	176.700	5.8	.04	.2	.1	112	1.5	1.7	6S0
95	87	3231312	49.69	38.125	176.692	5.7	.00	.2	.2	125	1.5	1.7	4S0
96	87	3231545	52.81	37.995	176.832	10.2	.05	1.0	.9	234	1.9	1.6	5S0
97	87	3231603	23.31	37.971	176.850	8.2	.00	.5	.3	233	1.6	1.6	4S0
98	87	3231701	36.10	38.063	176.762	5.2	.13	.3	.7	104	1.5	1.7	6S3
99	87	3231818	14.37	38.110	176.703	5.7	.03	.1	.1	114	1.9	1.9	6S1

No.	ORIGIN	YMDHM_Sec		LAT S	LON E	DEPTH	RMS	ERH	ERZ	GAP	Ma	Mc	ESN
100	87	3232059	54.75	37.991	176.877	6.4	.11	1.7	.8	257	2.2	2.3	5S1
101	87	3232322	32.65	38.056	176.750	9.2	.05	.2	.6	111	1.6	1.6	5S2
102	87	3232338	45.19	37.932	176.942	7.5	.07	1.4	1.6	286	2.7	2.3	7S0
103	87	3232345	5.50	38.057	176.759	6.4	.10	.4	1.7	110	2.3	2.4	7S1
104	87	3232357	12.23	38.025	176.758	8.7	.00	.4	1.0	164	1.6	1.6	4S0
105	87	3240011	15.73	38.053	176.760	8.0	.07	.3	.8	116	1.6	1.7	5S2
106	87	3240014	51.67	38.122	176.697	5.8	.07	.3	.3	160	1.8	1.9	6S1
107	87	3240100	57.24	38.053	176.770	5.8	.08	.4	.6	119	1.3	1.4	4S1
108	87	3240147	44.88	38.117	176.684	5.4	.13	.4	.5	140	2.3	2.2	7S1
109	87	3240356	48.25	38.074	176.740	2.4	.11	.3	4.7	83	2.1	2.2	8S1
110	87	3240449	38.34	38.137	176.690	2.3	.06	.3	.9	127	1.5	1.7	4S2
111	87	3240509	42.61	37.889	177.089	14.5	.07	8.1	1.1	312	2.2	1.7	5S0
112	87	3240601	15.73	38.156	176.704	.8	.08	.3	.3	159	1.6	2.0	6S2
113	87	3240747	27.50	37.839	176.489	2.9	.30	4.0	1.4	326	2.0	1.9	6S1
114	87	3240754	7.94	38.061	176.766	4.5	.07	.2	.8	113	2.1	2.2	8S2
115	87	3240840	10.35	38.068	176.745	5.5	.09	.3	.3	165	1.5	1.6	5S3
116	87	3240845	.65	37.948	176.904	8.5	.14	1.1	.8	258	2.1	2.1	8S3
117	87	3240846	10.95	37.932	176.916	.6	.21	3.1	1.9	266	1.9	2.0	7S2
118	87	3240903	22.58	38.039	176.772	5.3	.12	.5	.5	109	1.5	1.6	7S2
119	87	3241020	49.25	37.786	176.773	4.8	.17	32.3	4.1	317	1.7	1.9	4S0
120	87	3241029	17.60	37.933	176.818	6.0	.20	1.4	1.9	249	1.6	1.7	6S3
121	87	3241044	16.37	38.030	176.701	14.4	.03	.5	.7	222	1.4	1.4	4S1
122	87	3241137	17.05	38.122	176.695	9.7	.06	.7	.4	182	1.5	1.6	4S1
123	87	3241206	14.14	37.901	176.876	3.1	.00	1.2	.3	297	1.6	1.5	4S0
124	87	3241233	47.45	38.016	176.813	8.2	.09	1.2	1.3	186	1.2	1.2	4S1
125	87	3241250	2.16	37.765	177.068	10.1	.18	17.0	4.2	316	2.5	1.9	7S0
126	87	3241250	44.37	38.043	176.735	4.0	.10	.4	1.5	116	1.4	1.6	7S0
127	87	3241310	33.96	37.977	176.835	6.5	.33	2.1	2.5	223	1.4	1.5	5S3
128	87	3241317	46.91	37.951	176.858	4.7	.09	.7	.4	246	1.9	2.0	7S1
129	87	3241321	12.50	38.049	176.803	13.2	.32	1.7	3.4	126	1.4	1.3	4S2
130	87	3241323	3.36	37.970	176.781	4.9	.05	.5	.2	235	1.5	1.5	5S2
131	87	3241352	55.72	38.061	176.838	4.7	.04	.3	.3	148	1.7	2.5	4S1
132	87	3241418	37.51	37.947	176.863	10.1	.03	3.6	.6	270	1.4	1.7	4S0
133	87	3241520	51.93	38.117	176.700	7.5	.00	.2	1.0	176	1.5	1.6	4S0
134	87	3241734	10.11	38.164	176.686	9.9	.12	1.3	.9	216	1.6	1.5	4S2
135	87	3241802	8.96	38.013	176.794	5.4	.03	.3	.1	189	1.4	1.5	6S0
136	87	3241818	19.92	38.011	176.769	5.6	.02	.2	.2	191	1.4	1.5	4S1
137	87	3241839	58.51	38.009	176.825	8.0	.04	.5	.8	202	1.9	1.8	5S1
138	87	3241902	38.37	37.964	176.813	5.5	.05	.6	.2	251	1.5	1.6	5S2
139	87	3241912	51.71	38.167	176.690	10.0	.13	.5	.5	215	2.0	2.0	6S4
140	87	3242047	21.38	38.038	176.768	5.9	.19	1.0	.6	122	2.0	2.0	5S2
141	87	3242319	5.37	38.011	176.762	11.2	.12	1.6	1.2	192	1.9	1.7	4S2
142	87	3250501	40.21	38.042	176.773	10.2	.14	.9	1.3	122	1.9	1.9	6S1
143	87	3250659	38.53	38.009	176.833	2.7	.05	.5	.9	172	1.1	2.0	4S1
144	87	3250703	37.53	37.929	176.815	8.7	.18	1.4	1.0	252	1.4	1.5	7S1
145	87	3250725	8.62	38.054	176.775	2.6	.08	.3	2.8	130	1.4	1.6	6S1
146	87	3250758	48.84	38.041	176.783	5.5	.06	.3	.3	139	1.3	1.3	5S1
147	87	3250859	40.62	38.001	176.797	7.1	.11	.5	1.1	114	1.4	1.6	7S1
148	87	3250959	35.13	38.102	176.699	6.6	.02	.3	1.1	212	1.2	1.4	5S0
149	87	3251037	45.11	38.040	176.773	5.9	.07	.4	.4	138	1.4	1.4	5S1
150	87	3251301	58.41	38.036	176.781	5.5	.02	.2	.2	148	1.2	1.6	5S0

No.	ORIGIN YMDHM_Sec			LAT S	LON E	DEPTH	RMS	ERH	ERZ	GAP	Ma	Mc	ESN
151	87	3251427	49.86	37.980	176.792	9.5	.10	1.0	.5	114	1.2	1.2	5S0
152	87	3251522	5.32	38.001	176.821	12.3	.10	.9	1.6	181	1.8	1.7	5S0
153	87	3251639	36.92	37.977	176.818	6.7	.14	1.3	1.4	208	2.0	2.4	7S0
154	87	3251640	49.88	37.913	176.788	4.0	.00	1.0	.2	297	1.5	1.3	4S0
155	87	3251700	13.90	37.944	176.841	8.2	.14	1.1	1.4	246	1.6	1.7	7S1
156	87	3251701	31.08	37.913	176.868	2.6	.03	.8	.3	266	1.3	1.9	6S0
157	87	3251750	16.29	37.924	176.829	3.8	.13	.8	.8	257	1.8	2.0	6S1
158	87	3251844	51.70	38.053	176.781	6.0	.05	.3	.3	151	1.4	1.7	4S1
159	87	3251902	37.00	38.063	176.775	5.6	.10	.5	.3	136	1.8	2.0	6S1
160	87	3251940	31.93	37.902	176.900	3.5	.10	.8	.7	275	2.2	2.3	6S1
161	87	3252028	27.64	38.018	176.775	4.9	.08	.6	.4	178	1.3	1.4	5S2
162	87	3252143	36.76	38.056	176.794	6.8	.00	.3	.5	236	1.6	1.6	4S0
163	87	3252147	7.51	37.927	176.929	5.0	.04	1.9	.4	292	2.1	1.9	5S0
164	87	3252341	12.63	38.062	176.768	6.2	.00	.2	.7	165	1.0	1.4	4S0
165	87	3252342	3.75	38.056	176.769	6.7	.04	.3	1.3	136	1.1	1.3	5S0
166	87	3260635	37.52	37.858	176.974	12.6	.30	2.7	1.7	296	2.1	2.0	6S3
167	87	3260910	3.63	38.015	176.822	11.5	.02	1.8	2.2	127	1.3	1.4	4S0
168	87	3261028	51.76	37.871	176.911	13.8	.25	5.0	1.3	286	2.5	2.5	8S1
169	87	3261035	46.73	37.987	176.865	7.6	.24	1.5	2.3	231	2.2	2.9	7S1
170	87	3261142	40.37	38.049	176.773	8.4	.12	.6	1.1	154	1.3	1.5	6S3
171	87	3261153	28.21	37.941	176.889	6.4	.10	1.1	2.6	257	1.6	1.4	6S1
172	87	3261243	44.88	38.172	176.662	10.1	.18	4.6	2.8	256	1.8	1.6	6S0
173	87	3261354	43.78	38.028	176.783	8.1	.23	1.0	2.2	104	1.6	1.5	7S2
174	87	3261404	29.57	38.031	176.818	4.9	.11	2.6	2.8	123	1.3	1.5	5S1
175	87	3261504	57.21	38.187	176.615	12.6	.13	3.9	2.6	276	2.0	1.6	7S0
176	87	3261721	50.05	38.047	176.779	7.8	.28	1.2	3.0	122	1.2	1.4	7S1
177	87	3270112	2.36	37.936	176.816	5.4	.09	.7	.3	248	1.5	1.6	6S1
178	87	3270349	7.32	38.028	176.856	6.5	.22	1.0	1.1	136	1.5	1.7	7S3
179	87	3270551	43.50	38.067	176.757	6.7	.13	.4	1.3	83	1.3	1.6	7S2
180	87	3270630	19.96	38.210	176.636	8.2	.14	3.4	2.0	263	2.0	1.8	5S0
181	87	3270701	3.60	38.138	176.689	9.4	.11	.6	1.0	122	2.0	2.0	8S1
182	87	3270753	38.16	37.835	176.580	11.6	.21	11.6	1.6	312	2.0	2.0	9S0
183	87	3270915	44.07	37.991	176.793	12.3	.71	3.6	3.5	116	1.6	1.8	8S4
184	87	3270919	59.32	37.944	176.880	8.5	.12	1.3	1.4	276	1.4	1.4	6S1
185	87	3271013	46.53	37.980	176.742	8.0	.04	.6	.3	254	1.4	1.5	4S2
186	87	3271114	55.94	38.182	176.689	5.1	.10	1.4	.4	228	1.6	1.6	5S1
187	87	3271142	31.14	38.157	176.716	9.8	.00	.4	.5	151	1.4	1.6	4S0
188	87	3271208	25.03	38.010	176.819	8.5	.08	.4	.8	161	1.6	1.6	6S2
189	87	3271706	4.04	38.189	176.664	4.6	.14	1.7	.6	242	2.1	2.3	8S0
190	87	3271754	19.75	38.177	176.650	8.6	.16	1.0	1.4	239	2.0	1.9	8S1
191	87	3272019	22.15	38.049	176.779	6.3	.24	.6	4.8	103	1.5	1.6	7S1
192	87	3272148	8.00	38.137	176.679	5.2	.16	1.2	.7	201	1.9	2.0	6S1

Fig.4(a) Located aftershock epicenters on Mar.15

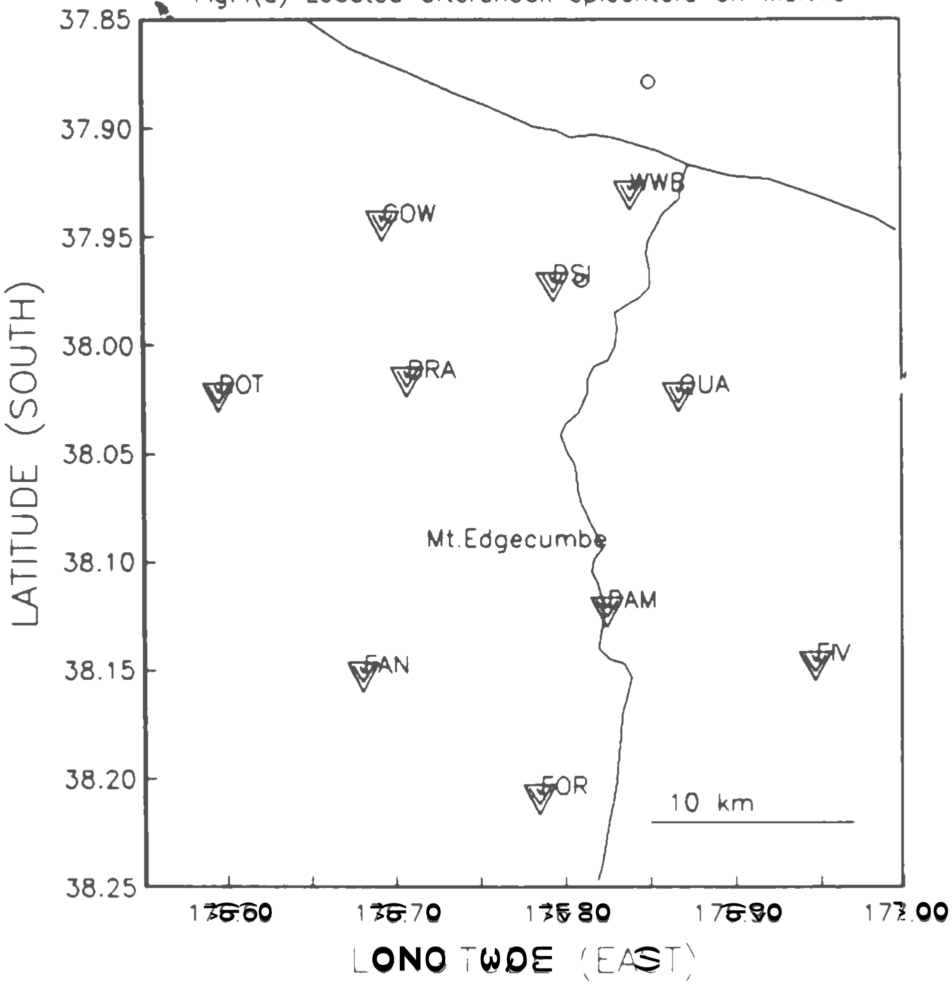

Fig.4(b) Located aftershock epicenters on Mar.16

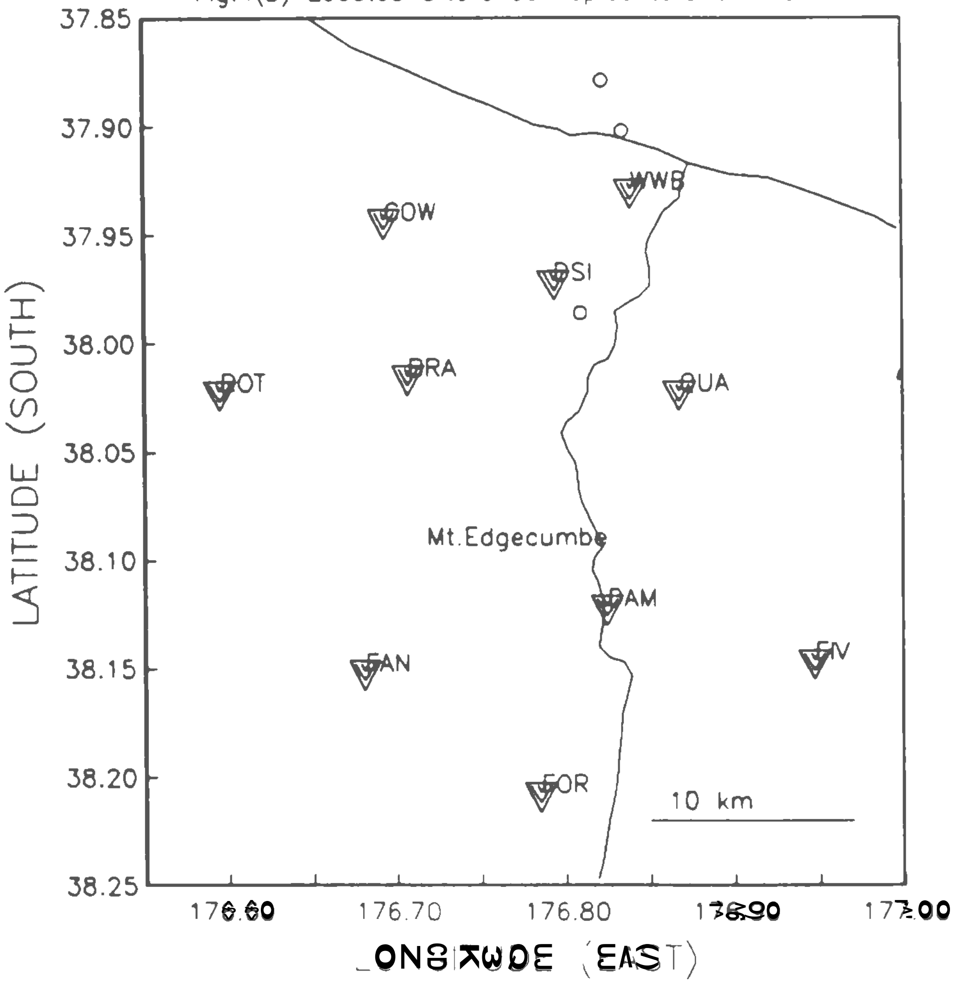

Fig.4(c) Located aftershock epicenters on Mar.17

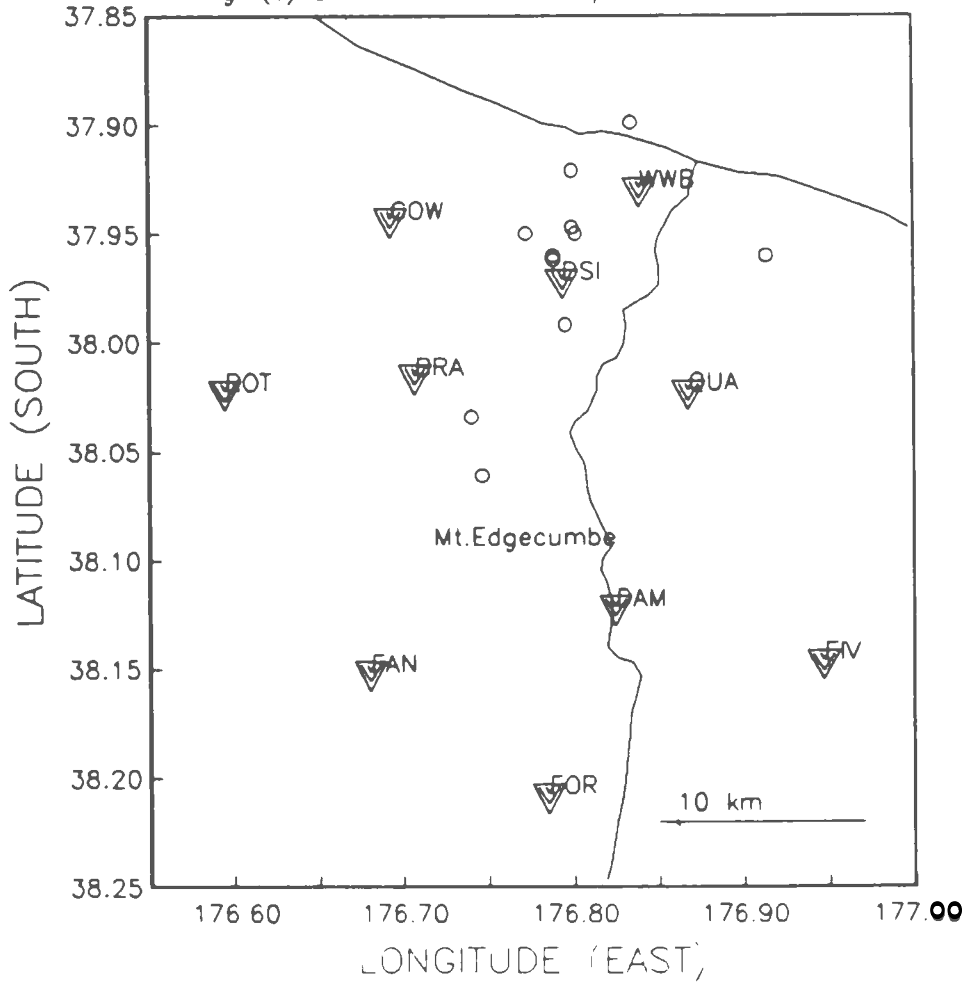

Fig.4(d) Located aftershock epicenters on Mar.18

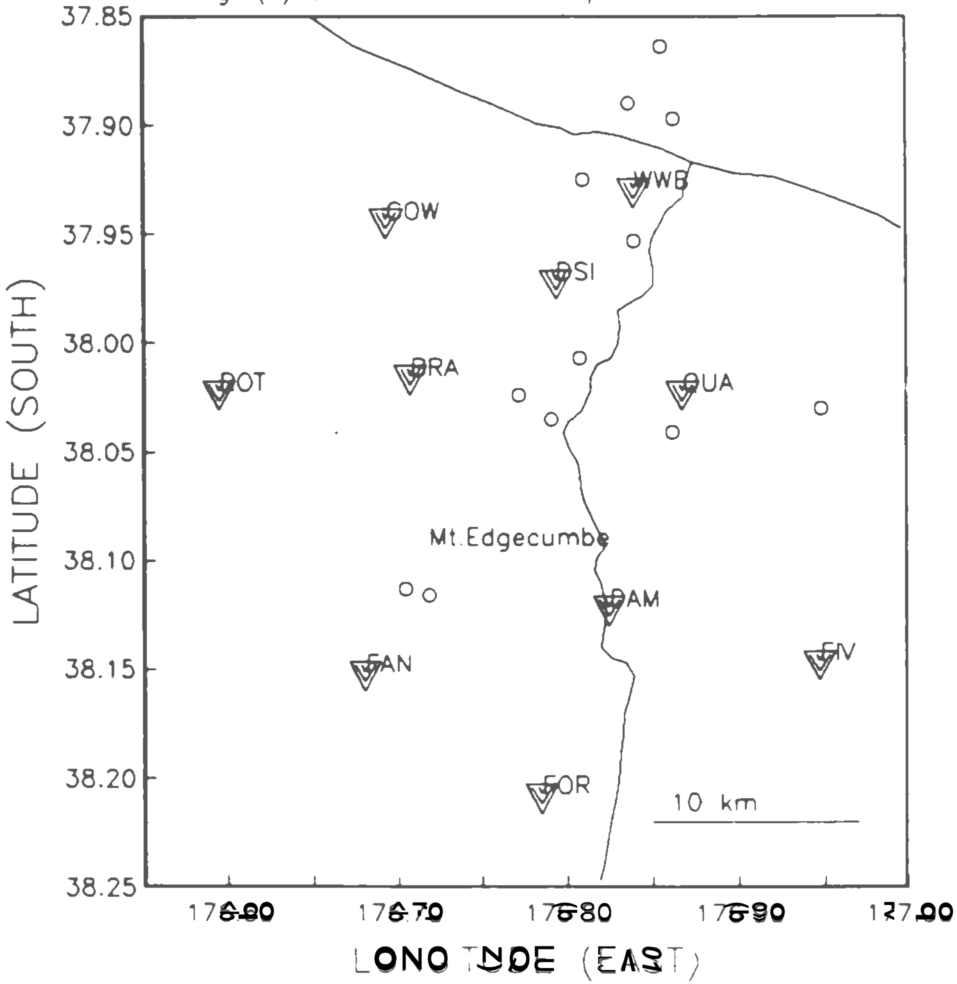

Fig.4(e) Located aftershock epicenters on Mar.19

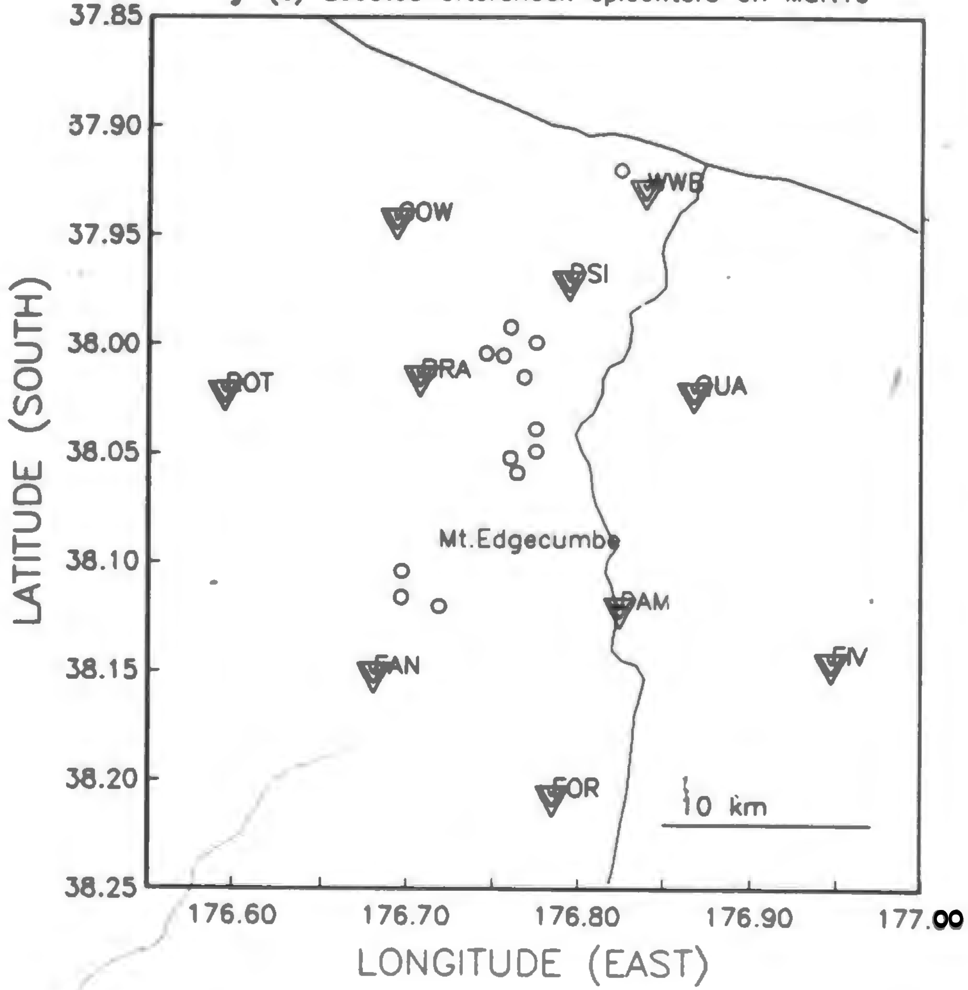

Fig.4(f) Located aftershock epicenters on Mar.20

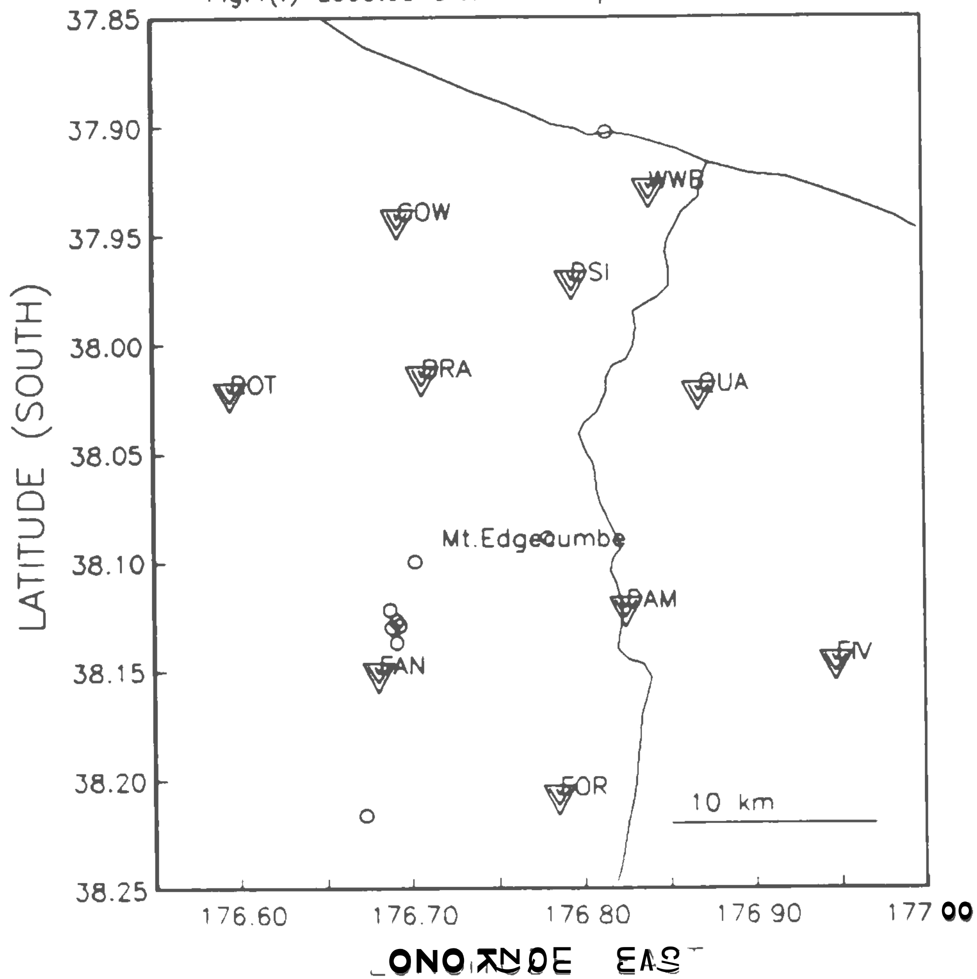

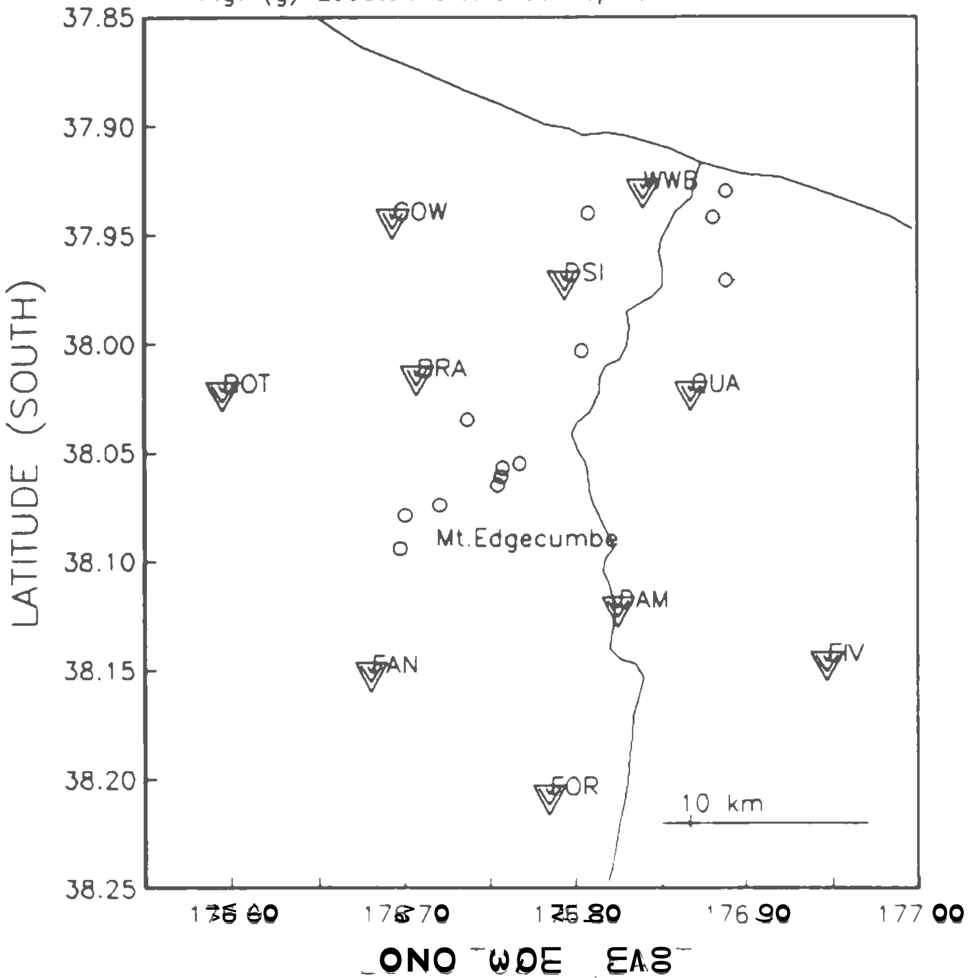

Fig.4(g) Located aftershock epicenters on Mar.21

Fig.4(h) Located aftershock epicenters on Mar.22

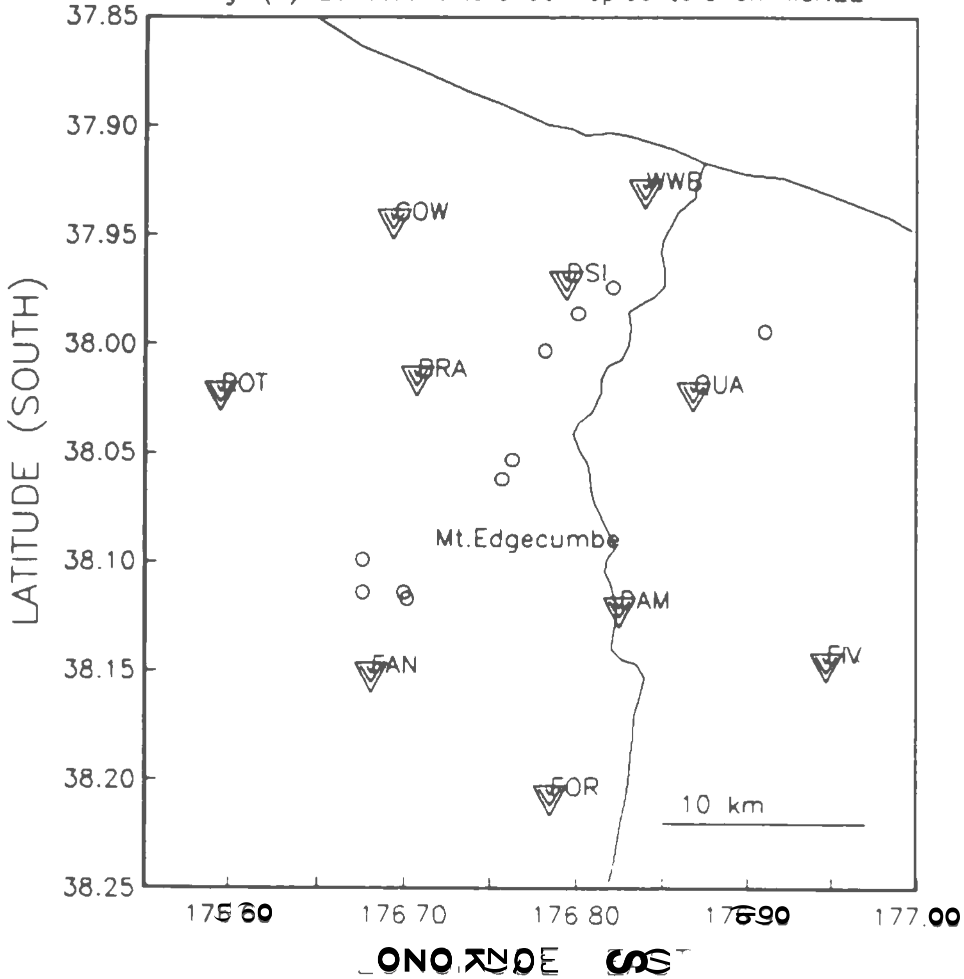

Fig.4(i) Located aftershock epicenters on Mar.23

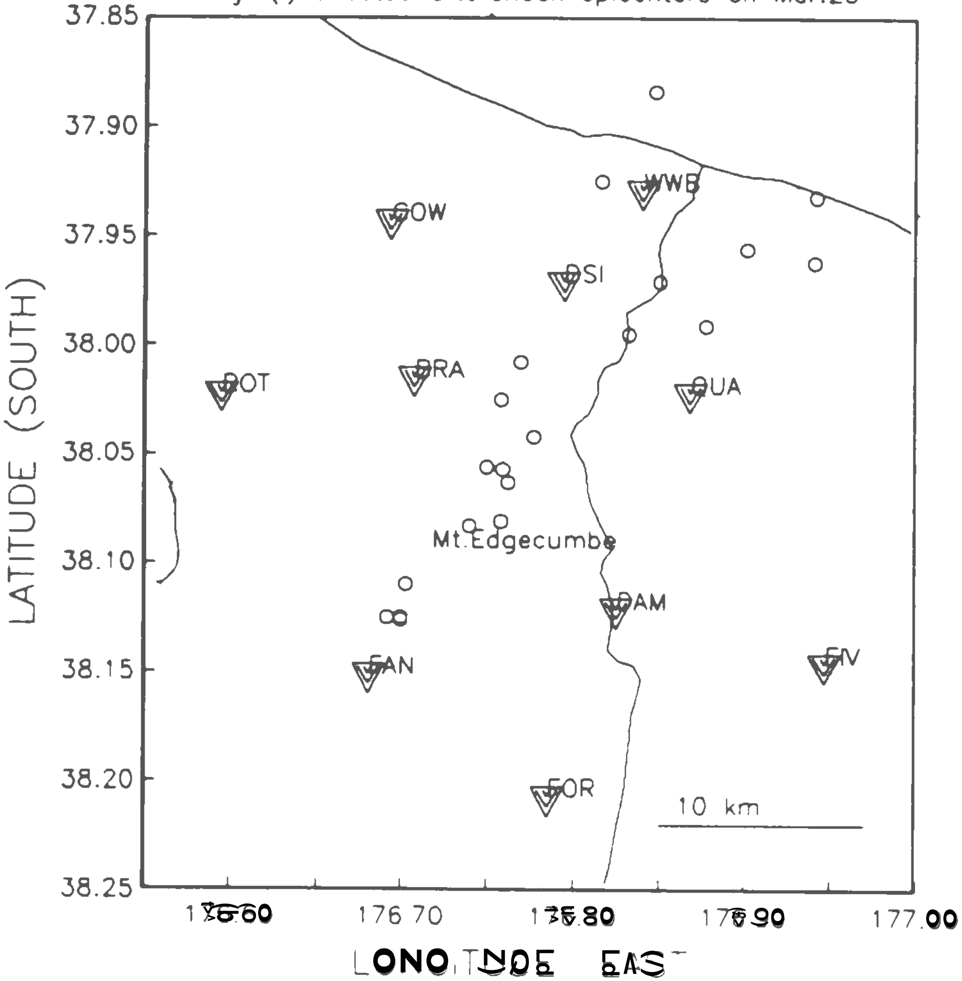

Fig.4(j) Located aftershock epicenters on Mar.24

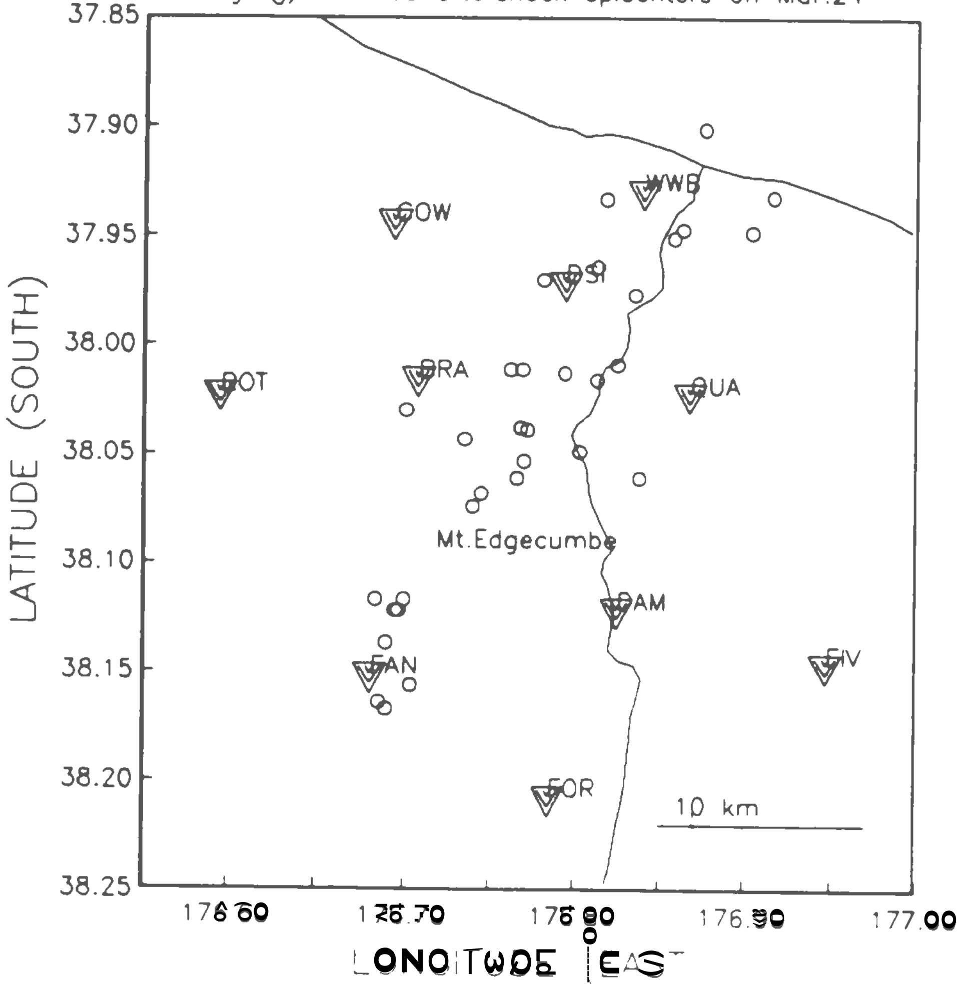

Fig.4(k) Located aftershock epicenters on Mar.25

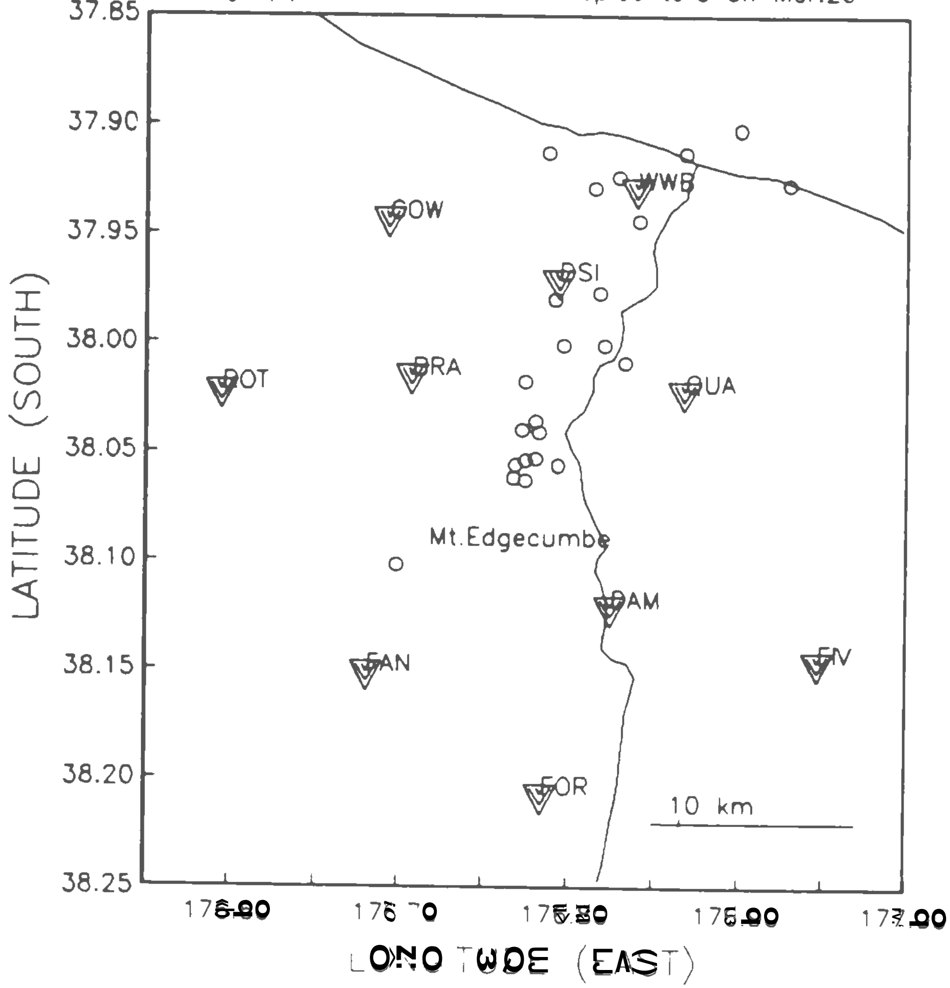

Fig.4(l) Located aftershock epicenters on Mar.26

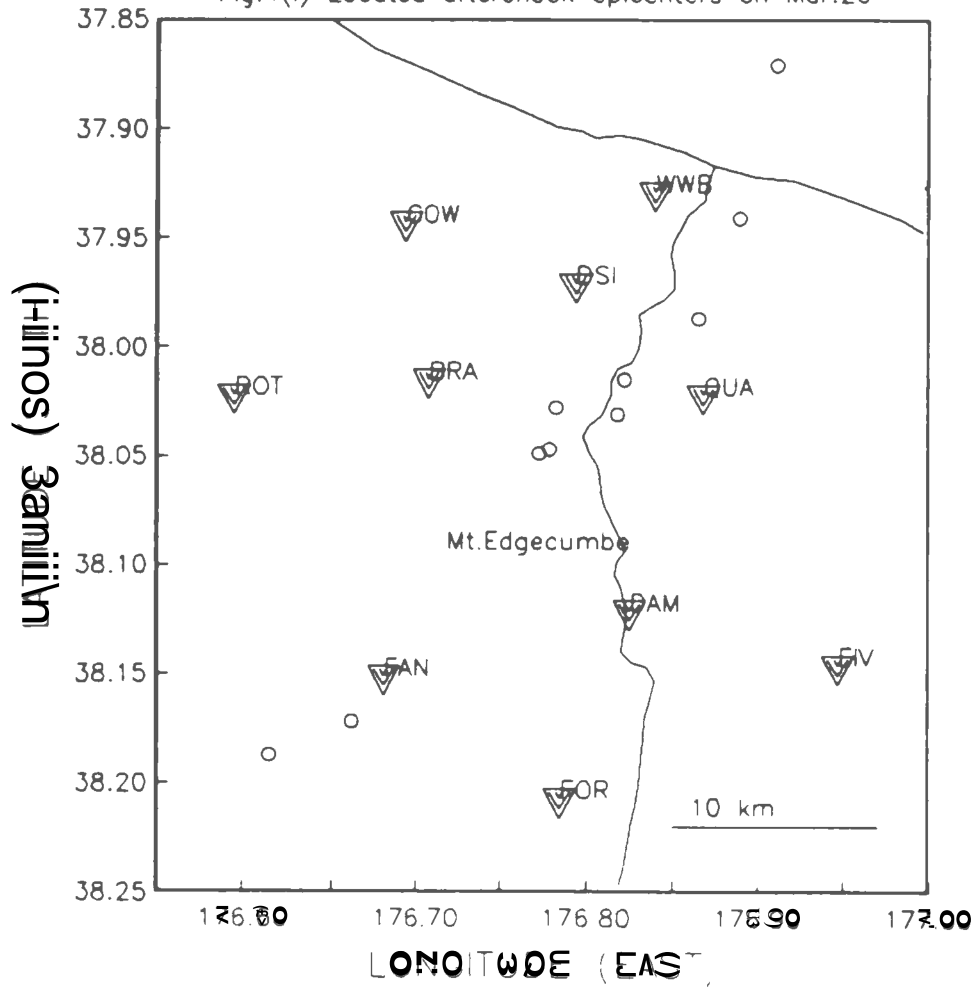

Fig.4(m) Located aftershock epicenters on Mar.27

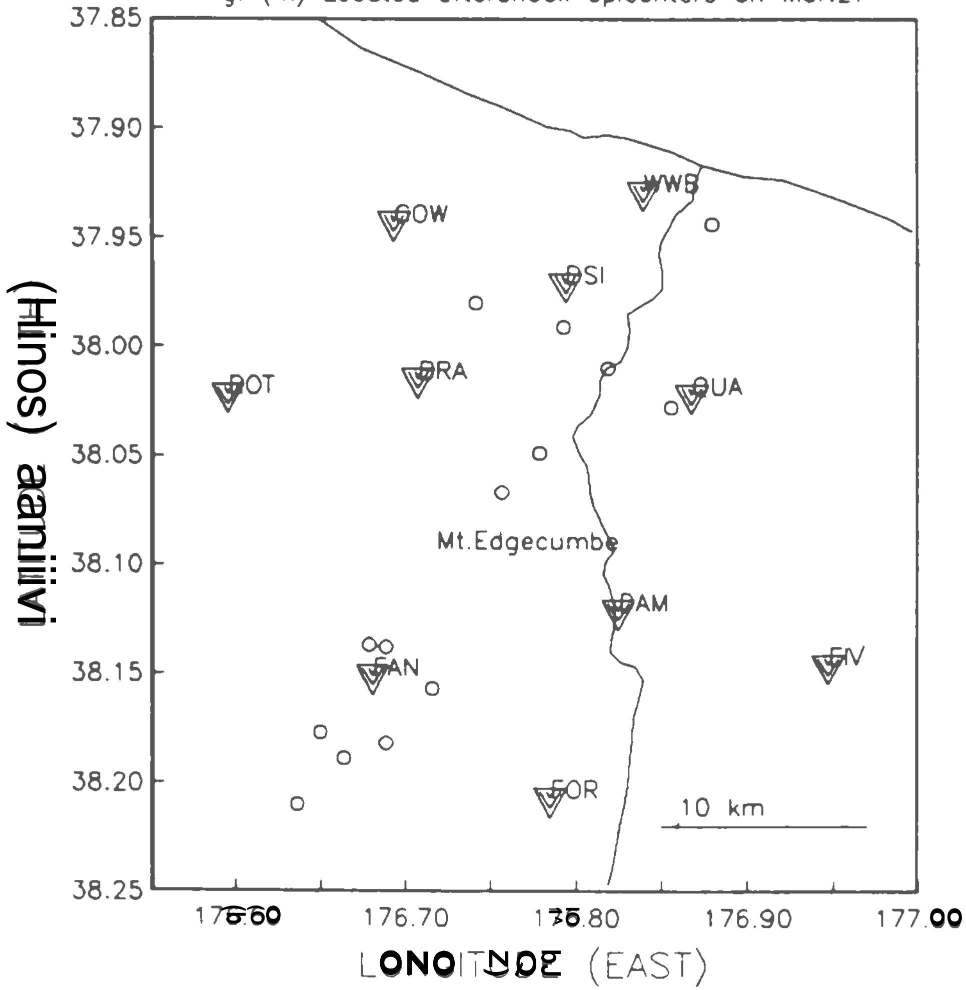

Figures 4(a-m) present the aftershocks on each day from Mar.15-27. There are no obvious changes in the pattern of epicenters form day to day.

A least squares fit to the spatial distribution of epicenters shows a N39°E trending direction (AA' in Figure 3). In this direction the later aftershock zone is at least 50 km long. In the southwestern part the epicenters are in a relatively narrow zone (<7 km) and they broaden to over 15 km wide in the northeast. Cross section projections of hypocenters at AA',BB',CC' as well as DD' are given in figure 5a,5b,5c,5d respectively.

On section AA', epicenters are distributed along about 50 km length. There are few epicenters shallower the 3 km, and few located deeper than 12 km. The number of deeper epicenters below Mt. Edgecumbe is decreased relative to other locations along this profile.

Section BB' shows possible subsurface projection of three faults that showed surface rupture after the main shock. The dip, 55 degree, is based on our focal mechanism result as well as previous inference by Nairn and Beanland (1989). The Edgecumbe fault, showing the greatest surface rupture, bisects the aftershock zone. There is no obvious relationship between the hypothesized fault geometry and the aftershock distribution. The later aftershock hypocenters do not define any fault plane, as noticed in the early aftershock study [Robinson 1989].

Mapped surface fault rupture in the region shown on section CC' are much shorter, and no mapped surface faulting occurred in the region on sectionDD'. Aftershocks in these region are less diffuse. There is a very weak suggestion of a dip to the northwest on section CC' and possibly a dip to the southeast on section DD'. However the trends are also too diffuse to confidently identify possible fault planes.

Most of the aftershocks presented in Table 2 have magnitude from 1.0 to 2.8 and a small number are a little less than 1.0. There are two magnitudes calculated: one from the peak to peak amplitude and the other from coda duration. Magnitude M_c is assumed proportional to the logarithm of coda duration and parameters are adjusted to be consistent with the moment magnitudes of 18 common events from digital recorders operated by the University of Nevada-Reno. Those moment estimations of the 18 events were derived from spectral analysis of records [Priestley: pers. comm. 1989] and the moment magnitudes were derived from the Kanamori magnitude-moment relationship [Hanks & Kanamori 1979].

The resultant relation we adopted to calculate coda magnitudes in our study is

$$\text{Coda Magnitude } M_c = 1.64*\log(D_r) - 0.26$$

where

D_r = Duration.

Those events which were recorded on smoke paper and also triggered digital recorders are relatively larger ones. For some of those events, amplitudes on smoke paper reached saturation. The total common events available are only 18. It is expected that there are big errors, because of the saturation, if we also directly use the moment magnitudes to adjust the parameters in magnitude-peak amplitude relationship. Instead amplitude magnitude is derived through the linear regression with the derived coda duration magnitude.

The resultant relation we adopted to calculate amplitude magnitudes in our study is

$$\text{Amplitude Magnitude } M_a = \log (A_m/2) + 0.8*\log (D_e^2 + D_p^2) - 0.6$$

where

D_e = Epicenter Distance;

D_p = Hypocenter Depth;

A_m = Peak to Peak Amplitude.

The figure 6a and 6b are the fitting lines showing the different magnitudes and the scattering situation.

Both magnitudes so derived are listed in the Table 2 (Event List). The obtained magnitudes of these later aftershocks are obviously smaller than the earlier aftershocks studied by Robinson (1989), most of which are greater than 3.0.

The magnitudes and event times are shown explicitly in Fig.7. The magnitude of each event in Fig.7 is the maximal one of amplitude and coda magnitudes for the event. The Fig.7 shows that the completeness of the record of located events compared with time and was at its best between March 23 and 26. For events above magnitude 1.8 there is some suggestion that the number of located events per day is gradually decreasing.

A histogram is given here (Figure 8) which shows most events are within 11 km of depth and aftershock number reaches a maximum near the depth of 6 km. This result is consistent with the main shock location which was estimated at 8 km depth and it agrees with the common situation that rupture usually initiates at the bottom of rupture area of faults for normal faulting [Jackson 1987].

From the epicenter distribution (Fig.3) there is obviously a gap between cluster DD' and CC'. The early aftershocks displayed a similar gap in same place [Robinson 1989]. The Holocene Mt. Edgecumbe volcano is in this gap and very high heat flow around that area is expected. The above seismic gap in the aftershock distribution may be caused by the high temperature there, which could prevent accumulation of elastic energy and only allow creep. The cross section along trending direction AA' provided another look of the gap. It seems that focal depth is getting more shallow when getting close to the gap. The events that apparently violate this trend are really projected in the gap from the side. This of course is in another way supporting our suggestion that the gap is due to the high temperatures associated with the volcano.

Fig.5a Cross section distribution along AA'.

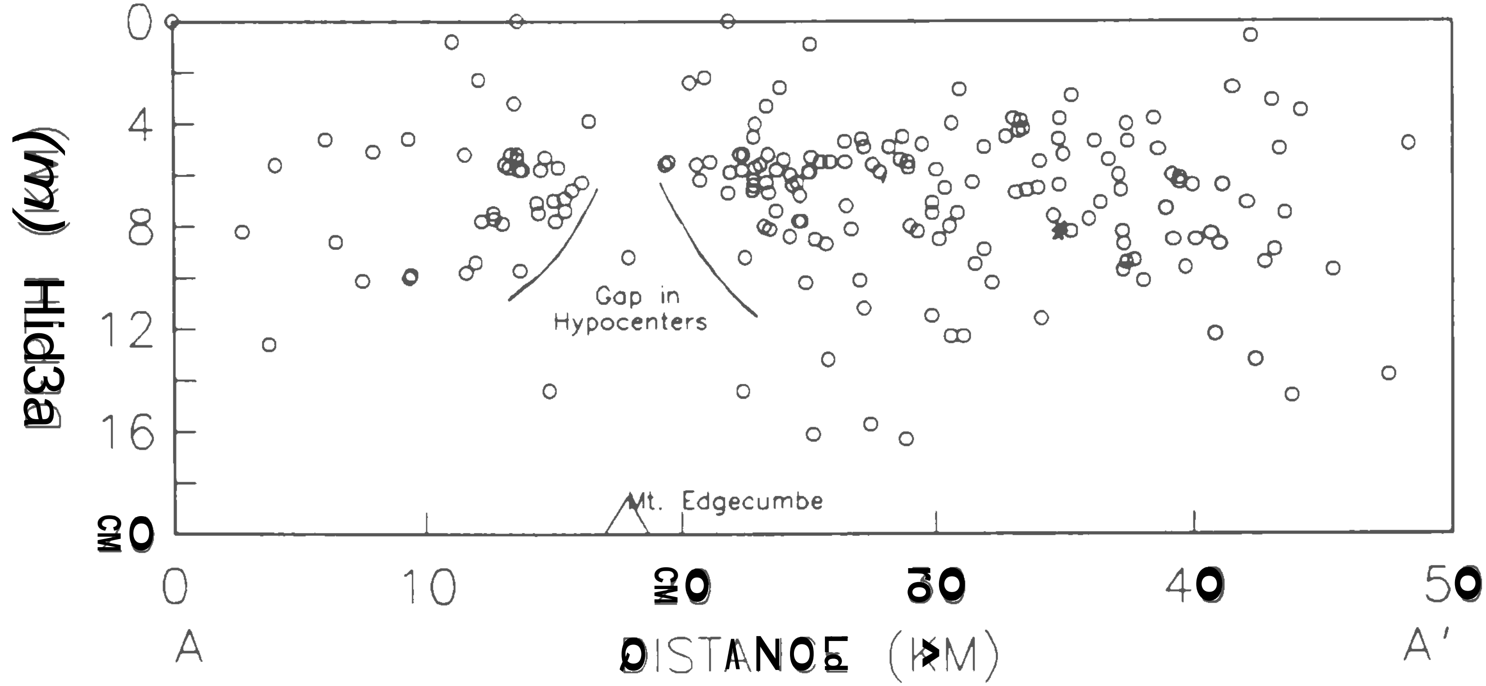

Fig. 3b Cross section distribution along BB'.

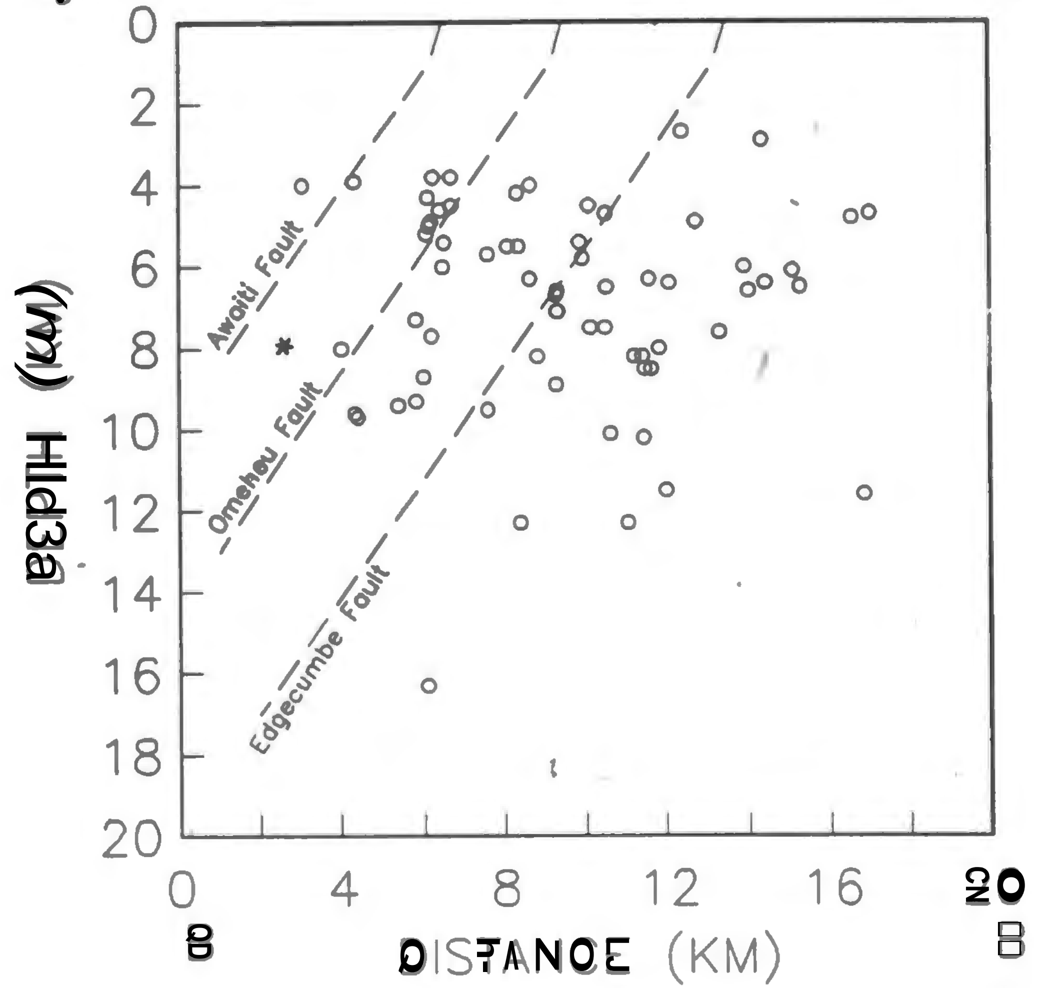

Fig.3 Cross section distribution along OO'.

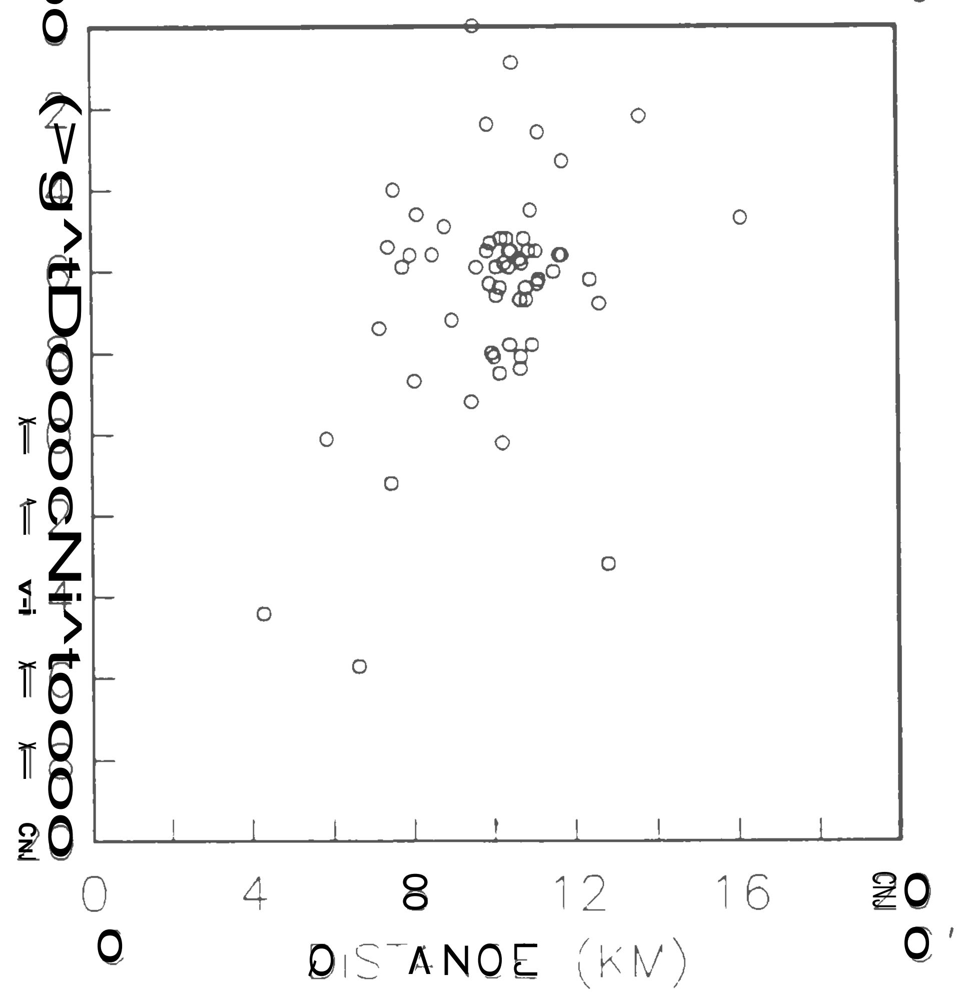

Fig.3d Cross section distribution along DD'.

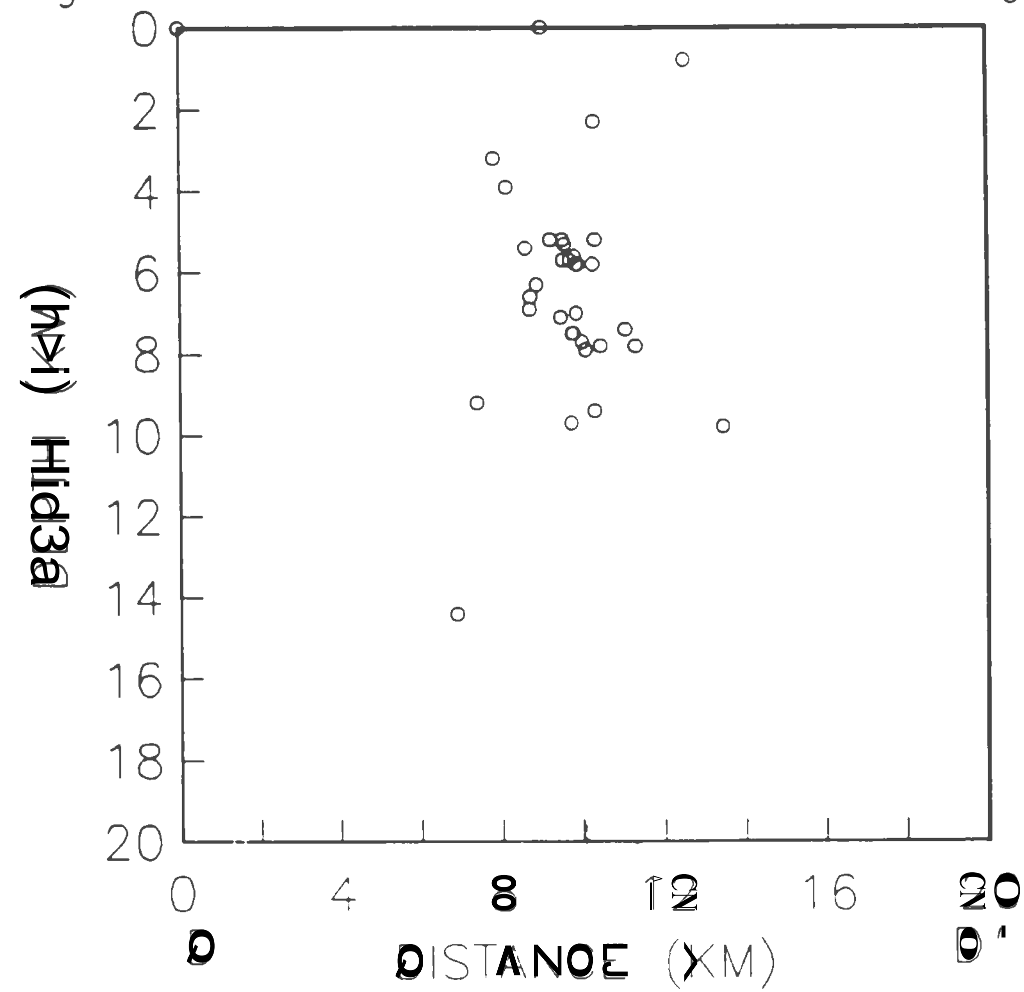

Fig.6a Coda duration magnitude vs moment and moment magnitude.

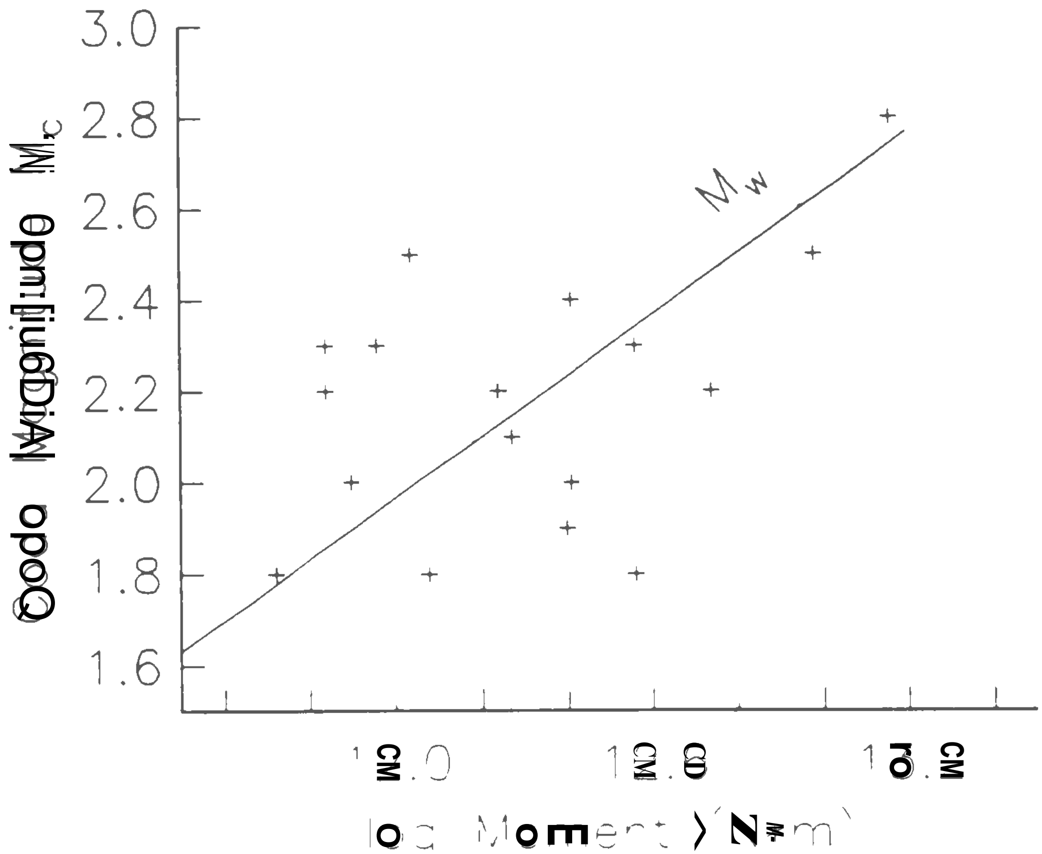

Fig.6b Amplitude magnitude vs
coda duration magnitude.

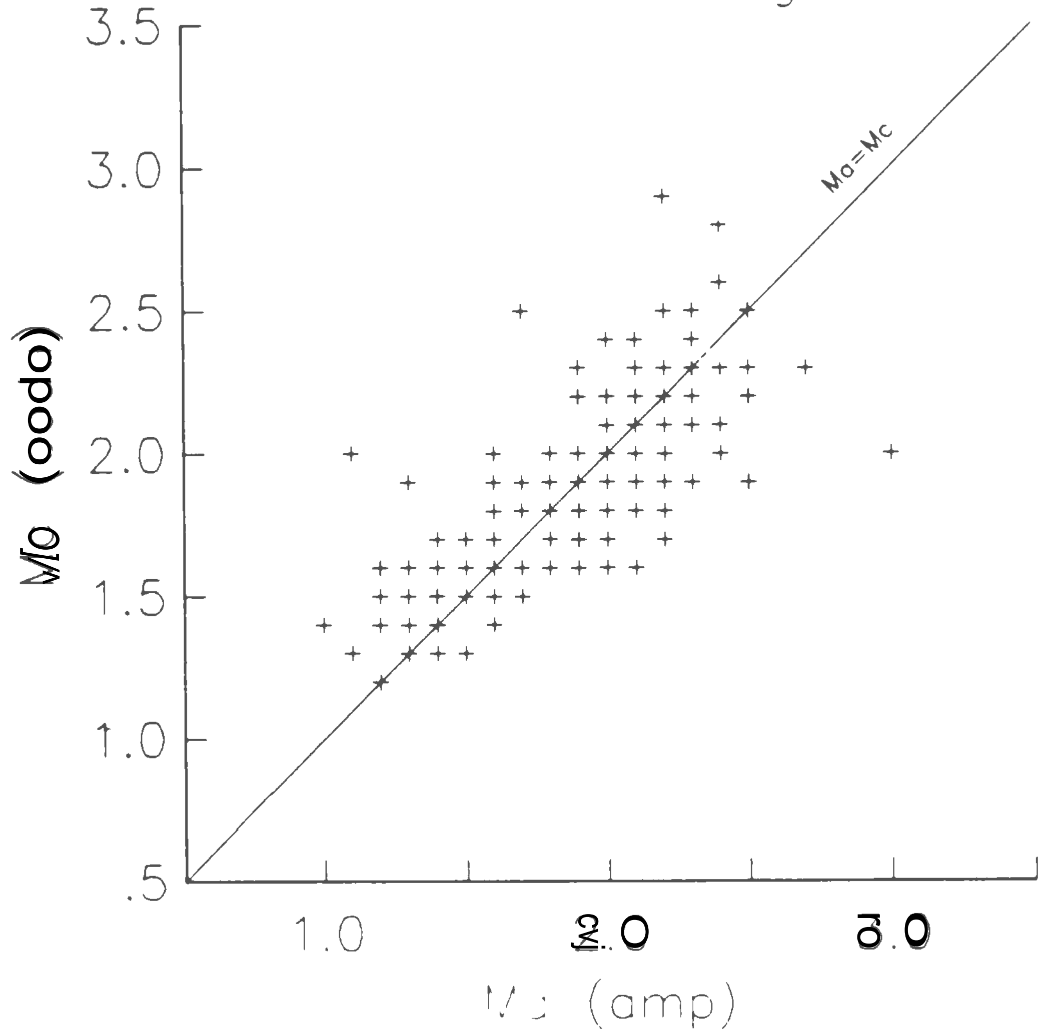

Fig.7 Magnitude vs Time

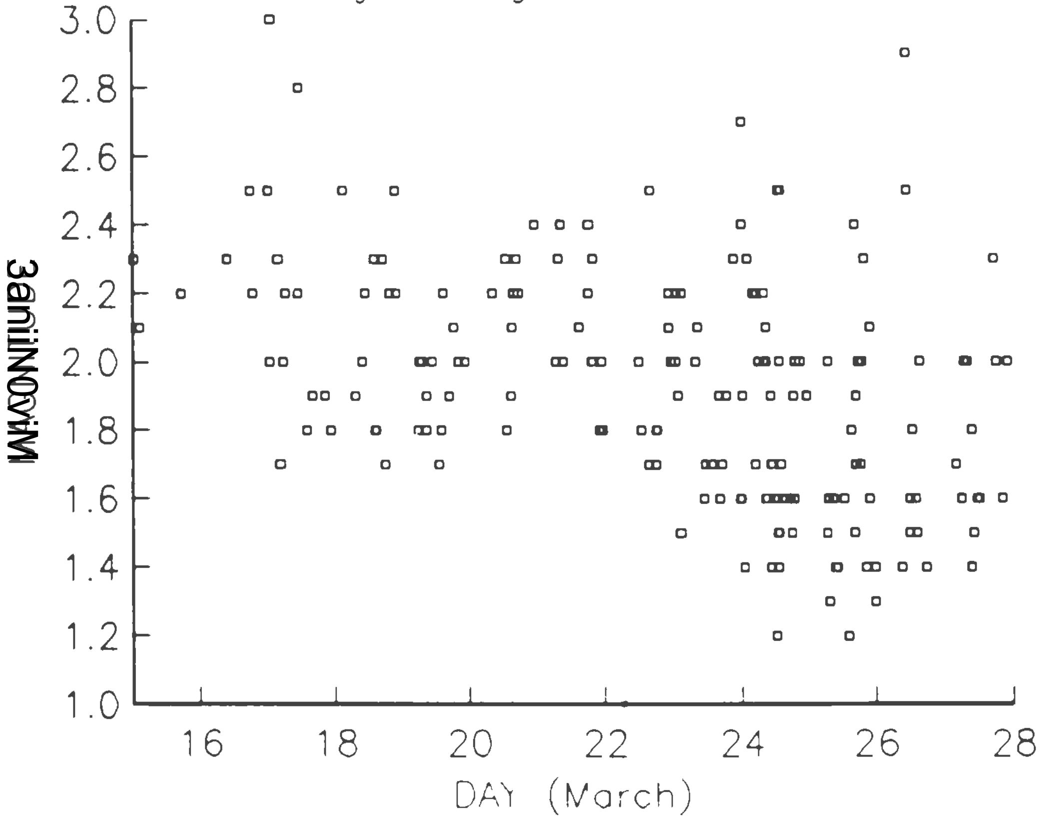

Fig.8 Histogram (Mar.15-27).

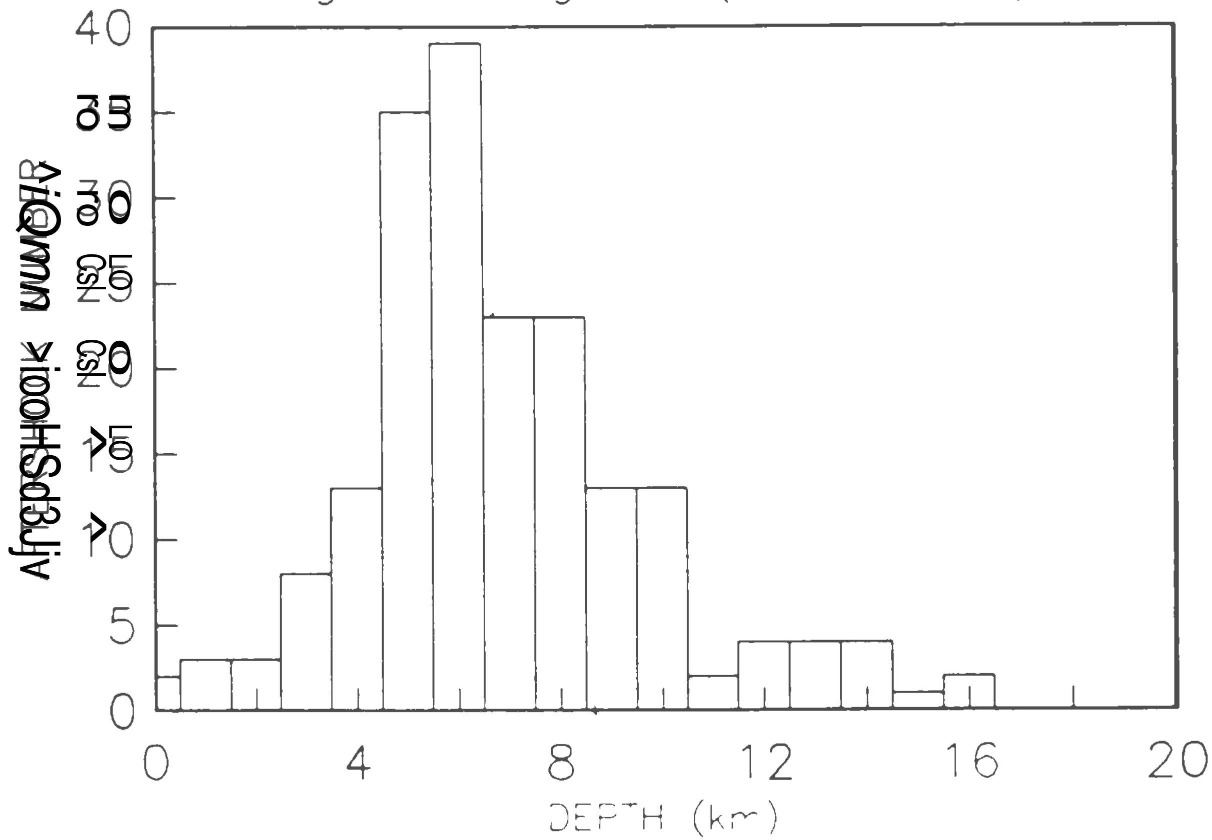

FOCAL MECHANISM

First arrival polarities (up or down) of all analyzed events were picked for focal mechanism analysis. Results are shown in Fig. 9. The stereographs are lower hemisphere. Darkened quarters represent compression (polarity Up) and white quarters represent dilatation (polarity Down). From the epicenter distribution, four clusters were selected to make a composite focal mechanism analysis. There is too much ambiguity to define the focal mechanism for most individual events due to the small number of effective stations for one aftershock. Figure 9 gives the four composite focal mechanisms corresponding to events in each square. A majority of events in a same square display a consistent focal mechanism with each other. The larger stereo graphs in figure 9 represent such predominant focal mechanism for their corresponding clusters. There are a small number of events in each cluster which can not be interpreted in the predominant focal mechanism. They are drawn separately to match their different mechanism, using smaller stereo balls. This deviation of focal mechanism is likely related to the complexity of faults in the area.

From the four predominant focal mechanism obtained, several features could be noticed. First of all they all fundamentally present normal faulting with very small strike slip component. Rake angles are larger than 75 degree from horizontal (less than 15 degree strike slipping component). Second, there is a small rotation of the T axis (Tension axis), toward a more north-south direction at the northern end of the aftershock zone. In our result the T axis rotates from 130° at south to near 155° at north (T axis angle is measured clockwise from due north direction).

Both the findings are supported by geological observations. Detailed pre- and post-earthquake field measurement had indicated the earthquake was a normal faulting. In addition a young terrace found right along the shore line might imply a northeast-southwest trending normal fault existing at the foot of terrace and parallel to the shore line [G. King: pers. comm. 1989]. This would be an active normal fault and downthrown seaward. It contributed to the formation of the terrace. If this is true the northern part of Whakatane graben would have some more extensional component in the north-south direction. Rotation of the T-axis in our aftershock focal mechanisms would be consistent with such a tendency. The terrace age was estimated at about 1,000 years and if the terrace is 10 m standing out from its foot the slip rate of the new fault would be on the order of 1 cm/year. The T axis direction geologically measured had a general agreement with our average result [Crook and Hannah 1989, Walcott 1984, Beanland at al 1989].

The percentage of events within the southern square which compose the predominant focal mechanism is somewhat higher than that in the northern square. Together with the characteristics of a more scattered epicenter distribution in the north it implies the faulting during the 1987 earthquake is more complicated in the north than in the south, where possibly only one single fault was involved in the earthquake. But in the north perhaps more small faults were involved during the faulting process of the main shock. In any case it appears that the diffuse distribution of aftershocks can only be consistent with activation of numerous small faults in the aftershock sequence. The numerous known or unknown active faults in Whakatane graben provided much possibility in the process.

Geological observations after the 1987 Edgecumbe earthquake made by Beanland at al [Beanland at al 1989] suggested the dip of the Edgecumbe fault which was the major rupture fault in the earthquake is probably 55°. Actually all available results from gravity analysis, seismic study and drillhole samples about dip angles of faults within the graben seem that they are not less than 35°. They are estimated around 45-55° [Anderson & Webb 1989, Nairn & Beanland 1989, Woodward 1989]. Most of surface ruptures in relatively northern part of the rupture zone were observed downthrown to northwest. So fault planes in the top three major stereo balls should be the northwest dipping nodal planes. In such a way, their dip angles are about 40-55°, agreeing with observations. But in the bottom stereo ball if the northwest dipping nodal plane is interpreted as fault plane its dip angle is only 30°, which is too small compared to the various results above. The cross section in figure 5d which corresponds to the same cluster of aftershocks also is more consistent with a steeply dipping fault downthrown to the southeast than with a shallow-dipping fault plane downthrown to the northwest, although that clue is weak. Thus the corresponding focal mechanism could be explained that the southeast-dipping nodal plane is the fault plane which now is downthrown to southeast and has a dip angle 55°. In field observation there are surface breaks in the relatively southern part of the rupture zone which were indeed found downthrown to southeast (Rotoitipakau faults, Fig. 1). Those Rotoitipakau fault surface ruptures are located northwest of Mt. Edgecumbe while the southern aftershock cluster is located southeast to the Mt. Edgecumbe. Extrapolation of those surface ruptures, however, allow the possibility that maybe the Rotoitipakau fault or related southeast dipping fault, extend more underneath to the south. If so, they could more reasonably on geometry contribute to the aftershocks in the southern one cluster. Another suggestion is of course also possible to explain the southeast downthrown focal mechanism: different faults having no surface breaks under the southern cluster location may also be the source of those aftershocks. The data has not had any certain answer to this problem.

With the fault planes so determined the strike direction shown by the four major stereo balls is ranging from 40 to 70 degree northeast. The surface rupture observations are consistent with this.

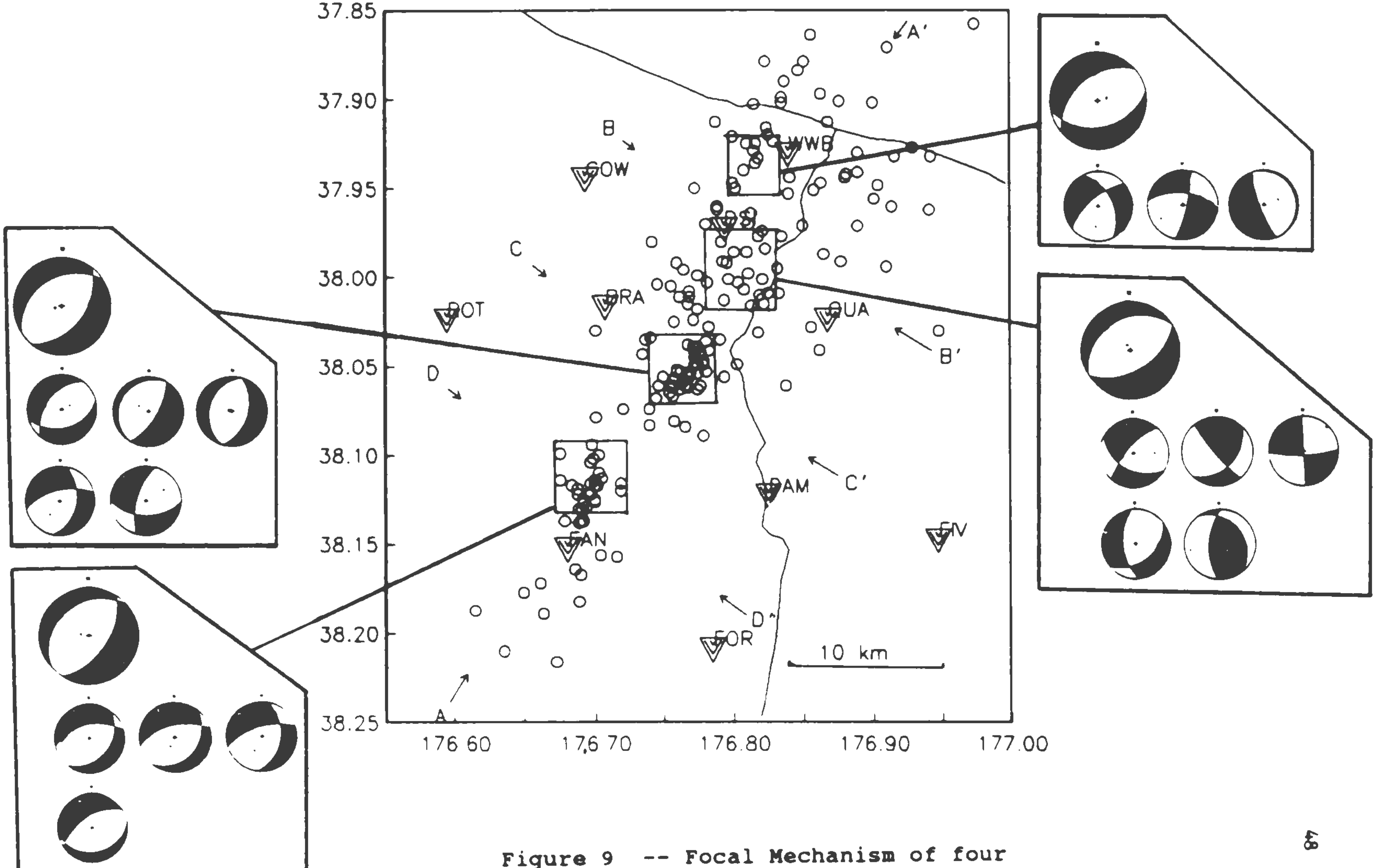

Figure 9 -- Focal Mechanism of four aftershock clusters

CONCLUSION

Aftershocks showed again that the 1987 Edgecumbe earthquake was a shallow normal faulting earthquake with a small (15 degree on average) strike slip component. Predominant focal mechanism presented the faulting with average N50°E strike, and 50° dip to the northwest for northern part and 55° dip to southeast for the southern part of the aftershock zone. Aftershock epicenter distribution scattered at least to 15 km wide area and focal mechanism displayed more complicated property in the northern part of the aftershock zone, probably caused by more small active faults than we thought involved in the 1987 Edgecumbe earthquake main shock faulting process. The southern part of the aftershock zone is relatively more simple. There aftershocks concentrated in an area only 7 km wide and focal mechanisms showed relatively more identity. It means probably only one single fault contributed to the aftershocks there, which as revealed is also a normal fault but dipping into southeast. Extensional axis has more north-south component on the zone close to the sea shore.

An aftershock epicenter distribution gap is present under Mt. Edgecumbe, and might becaused by very high heat flow near Mt. Edgecumbe.

Overall our study of later aftershocks of the 1987 Edgecumbe earthquake has provided new evidences which generally are consistent with the geological observations in that region. The earthquake was the continuation of the process of Whakatane graben subsiding and extending.

It should be said that all of our results are not surprising for that extensional back arc graben with thin crust, high heat flow and active recent volcanic activity.

REFERENCES

Anderson, H. and T. Webb,"The Rupture Process of the Edgecumbe Earthquake, New Zealand", New Zealand Journal of Geology & Geophysics, Vol.32, No.1, 1989, pp.43-52.

Beanland, S.,Kevin R. Berryman and Graeme H. Blick,"Geological Investigations of the 1987 Edgecumbe Earthquake, New Zealand", New Zealand Journal of Geology & Geophysics, Vol.32, No.1, 1989, pp.73-92.

Cole, J. W. (1979),"Structure, Petrology and genesis of Cenozoic Volcanism, Taupo Volcanic Zone, New Zealand--A Review.", New Zealand Journal of Geology & Geophysics, Vol.22, pp.631-657.

Crook, C. N. and J. Hannah,"Regional Horizontal deformation Associated with the 1987 Edgecumbe Earthquake, Bay of Plenty, New Zealand - An Introduction", New Zealand Journal of Geology & Geophysics, Vol.32, No.1, 1989, pp.93-98.

Crosson, R. S. (1976),"Crustal Structure and Modelling of Earthquake data,1: Simultaneous Least Squares Estimation of Hypocenters and Velocity Parameters.", J. Geophys. Res., Vol. 81, pp3036-3046.

Hanks, T. C. and Kanamori, H. (1979),"A Moment magnitude Scale", J. Geophys. Res., Vol.84, pp2348-2350.

Jackson, J. A. (1987),"Active Normal Faulting and Crustal Extension", in: Croward, M.P., Dewey, J.F. and Hancock, P.L. ed. Continental Extension Tectonics. Geological Society special publication, Vol.28, pp.3-17.

Klein, F. W. (1978),"Hypocenter Location Program: HYPOINVERSE", US Geological Survey Open File 78-694.

Nairn, I. A. (1976),"Late Quaternary Faulting in the Taupo Volcanic Zone.", in Nathan, S. ed. Comp. Excursion Guide, No. 55A and 55C, 25th International Geological Congress.

Nairn, I. A. and Sarah Beanland (1989),"Geological Setting of the 1987 Edgecumbe Earthquake, New Zealand", New Zealand Journal of Geology & Geophysics, Vol.32, No.1, 1989, pp.1-14.

Robinson, R.,"Aftershocks of the 1987 Edgecumbe Earthquake, New Zealand: Seismological Structural Studies Using Portable Seismographs in the Epicenter region", New Zealand Journal of Geology & Geophysics, Vol.32, No.1, 1989, pp.61-72.

Priestley, Keith (1989),"Source Parameters of the 1987 Edgecumbe Earthquake, New Zealand", New Zealand Journal of Geology & Geophysics, Vol.32, No.1, 1989, pp.53-60.

Staff of New Zealand Department of Scientific and Industrial Research (1987),"The 1987 March 2 Earthquake near Edgecumbe, North Island, New Zealand", EOS Transactions of the American Geophysical Union, Vol.68, pp.1162-1171.

Studt, F. E. and Thompson, G. E. K. (1969),"Geothermal Heat Flow in the North Island of New Zealand.", New Zealand Journal of Geology & Geophysics, Vol.12, pp.673-683.

Stern, T. A. (1985),"A Back-Arc Basin Formed within Continental Lithosphere: The Central Volcanic Region of New Zealand.", Tectonophysics, Vol.112, pp.385-409.

Walcott, R. I. (1984),"The Kinematics of the Plate Boundary Zone through NewZealand: A Comparison of Short- and Long-Term Deformations", Geophysical Journal of Royal Astronomical Society, Vol.79, pp.613-633.

Woodward, D. J.,"Geological Structure of the Rangitaiki Plains near Edgecumbe, Nea Zealand, from Seismic Data", New Zealand Journal of Geology & Geophysics, Vol.32, No.1, 1989, pp.15-16.